International Journal of Systems Science

ISSN: 0020-7721 (Print) 1464-5319 (Online) Journal homepage: http://www.tandfonline.com/loi/tsys20

Tightly coupled long baseline/ultra-short baseline integrated navigation system

Pedro Batista, Carlos Silvestre & Paulo Oliveira

To cite this article: Pedro Batista, Carlos Silvestre & Paulo Oliveira (2016) Tightly coupled long baseline/ultra-short baseline integrated navigation system, International Journal of Systems Science, 47:8, 1837-1855, DOI: 10.1080/00207721.2014.955070

To link to this article: http://dx.doi.org/10.1080/00207721.2014.955070

International Journal of Systems Science, 2016
Vol. 47, No. 8, 1837–1855, http://dx.doi.org/10.1080/00207721.2014.955070

Taylor & Francis
Taylor & Francis Group

Tightly coupled long baseline/ultra-short baseline integrated navigation system

Pedro Batista[a,*], Carlos Silvestre[a,b] and Paulo Oliveira[a,c]

[a]*Institute for Systems and Robotics, Instituto Superior Técnico, Universidade de Lisboa, Lisboa, Portugal;* [b]*Department of Electrical and Computer Engineering, Faculty of Science and Technology, University of Macau, China;* [c]*Department of Mechanical Engineering, Instituto Superior Técnico, Universidade de Lisboa, Lisboa, Portugal*

(*Received 24 September 2013; accepted 2 April 2014*)

This paper proposes a novel integrated navigation filter based on a combined long baseline/ultra short baseline acoustic positioning system with application to underwater vehicles. With a tightly coupled structure, the position, linear velocity, attitude, and rate gyro bias are estimated, considering the full nonlinear system dynamics without resorting to any algebraic inversion or linearisation techniques. The resulting solution ensures convergence of the estimation error to zero for all initial conditions, exponentially fast. Finally, it is shown, under simulation environment, that the filter achieves very good performance in the presence of sensor noise.

Keywords: navigation; marine robotics; long baseline; ultra-short baseline; observability analysis; sensor fusion

1. Introduction

Navigation systems are vital for the successful operation of autonomous vehicles. For aerial and ground vehicles, the much celebrated global positioning system (GPS) is the usual choice, warranting aided navigation solutions such as the ones presented in Sukkarieh, Nebot, and Durrant-Whyte (1999), Vik and Fossen (2001), and Batista, Silvestre, and Oliveira (2009), see also the references therein. In underwater scenarios, other solutions must be devised due to the high attenuation that the electromagnetic field suffers. In particular, long baseline (LBL) and short baseline (SBL) acoustic positioning systems have been employed, see e.g. Whitcomb, Yoerger, and Singh (1999), Jouffroy and Opderbecke (2004), Kinsey and Whitcomb (2003), Larsen (2000), Vaganay, Bellingham, and Leonard (1998), Ricordel, Paris, and Opderbecke (2001), and references therein. Another commercially available solution is the GPS Intelligent Buoy (GIB) system, see Thomas (1998). Further work on the GIB underwater positioning system can be found in Alcocer, Oliveira, and Pascoal (2007). Position and linear velocity globally asymptotically stable (GAS) filters based on an Ultra-Short Baseline (USBL) positioning system were presented by the authors in Batista, Silvestre, and Oliveira (2010a), while the extended Kalman filter (EKF) is the workhorse of the solution presented in Morgado, Oliveira, Silvestre, and Vasconcelos (2006). For interesting surveys on underwater navigation, please see Leonard, Bennett, Smith, and Feder (1998) and Kinsey, Eustice, and Whitcomb (2006).

The GPS, LBL, SBL, USBL, or GIB positioning systems are essentially employed in the estimation of linear motion quantities (position, linear velocity, acceleration) and other sensors are usually considered for the problem of attitude estimation, which is still a very active area of research, as evidenced by numerous recent publications, see e.g. Metni, Pflimlin, Hamel, and Soueres (2006), Tayebi, McGilvray, Roberts, and Moallem (2007), Campolo, Keller, and Guglielmelli (2006), Choukroun (2009). The EKF has been instrumental to many stochastic solutions, see e.g. Sabatini (2006), while nonlinear alternatives, aiming for stability and convergence properties, in deterministic settings, have been proposed in Sanyal, Lee, Leok, and McClamroch (2008), Vasconcelos, Cunha, Silvestre, and Oliveira (2007), Rehbinder and Ghosh (2003), Mahony, Hamel, and Pflimlin (2008), Thienel and Sanner (2003), Grip, Fossen, Johansen, and Saberi (2012), and Martin and Salaun (2010), to mention just a few, see Crassidis, Markley, and Cheng (2007) for a thorough survey on attitude estimation. Recently, the authors have proposed two alternative solutions in Batista, Silvestre, and Oliveira (2012a) and Batista, Silvestre, and Oliveira (2012c). In the first, the Kalman filter is the workhorse, where no linearisations are carried out whatsoever, resulting in a design which guarantees globally asymptotically stable (GAS) error dynamics. In the latter, a cascade observer is proposed that achieves globally exponentially stable (GES) error dynamics and that requires less computational power than the Kalman filter, at the expense of the filtering performance.

* Corresponding author. Email: pbatista@isr.ist.utl.pt

Common to both solutions is the fact that the topological restrictions of the Special Orthogonal Group $SO(3)$ are not explicitly imposed, though they are verified asymptotically in the absence of noise. In the presence of sensor noise, the distance of the estimates provided by the cascade observer or the Kalman filter to $SO(3)$ remains close to zero and methods are proposed that give estimates of the attitude arbitrarily close to $SO(3)$. In Batista, Silvestre, and Oliveira (2012b) an alternative additional result gives attitude estimates explicitly on $SO(3)$, at the possible expense of the continuity of the solution during the initial transients, hence not violating the topological limitations that are thoroughly discussed in Bhat and Bernstein (2000).

For underwater vehicles, the usual sensing devices employed for attitude determination are two triads of orthogonally mounted accelerometers and magnetometers, coupled with a triad of orthogonally mounted rate gyros, used for filtering purposes. Essentially, the magnetometers and the accelerometers provide direct measurements, in body-fixed coordinates, of known vectors in inertial coordinates. Hence, an attitude estimate can be readily obtained from the solution of the Wahba's problem. With additional angular velocity measurements, it is then possible to design attitude filters, possibly including the estimation of rate gyro bias. The disadvantage of the use of magnetometers is that they are subject to magnetic field anomalies, such as the ones that can be encountered nearby objects with strong magnetic signatures, rendering the magnetic field measurements position dependent and therefore useless. This can be particularly dangerous in underwater intervention scenarios and as such alternatives need to be devised.

In previous work by the authors, see Batista, Silvestre, and Oliveira (2011a), a novel complete navigation system was proposed based on a combined Long Baseline / Ultra-short Baseline (LBL/USBL) acoustic positing system. With an LBL acoustic positioning system, an underwater vehicle has access to the distances to a set of known transponders, which are usually fixed in the mission scenario. Under some mild assumptions on the LBL configuration, it is possible to determine the inertial position of the vehicle. With an Ultra-Short Baseline acoustic position system installed onboard the vehicle, in the so-called inverted configuration, see Morgado, Batista, Oliveira, and Silvestre (2011), the vehicle has access to the distance to a fixed transponder in the mission scenario and the time (or range) differences of arrival between each pair of receivers of the USBL array. From those measurements, and under some mild assumptions on the USBL array configuration, the position of the external landmark relative to the vehicle, expressed in body-fixed coordinates, is readily available. Using spread spectrum techniques, see Morgado, Oliveira, and Silvestre (2010), it is possible to combine LBL and USBL acoustic positioning devices, which gives, in essence, both the distance between the vehicle and each of the external landmarks and the time (or range) differences of arrival between pairs of receivers, for each landmark. In this way, with an LBL/USBL it is not only possible to determine the inertial position of the vehicle but also the positions of the external LBL landmarks with respect to the vehicle, expressed in body-fixed coordinates. In Batista et al. (2011a), and for attitude determination purposes, the latter were employed to obtain body-fixed vector measurements of known constant inertial vectors, hence allowing for attitude estimation, while the inertial position was used to the estimation of the linear motion quantities.

The actual measurements of an LBL/USBL acoustic positioning system are acoustic signals, which when processed yield ranges and range differences of arrival (RDOA) between the acoustic receivers of the USBL. In Batista et al. (2011a) these were used, resorting to inversion or algebraic optimisation techniques, to obtain the inertial position of the vehicle and the body-fixed positions of the landmarks. However, it would be beneficial if the actual range and RDOA could be directly employed in the estimation solution, avoiding intermediate nonlinear computations that can distort noise and allowing for better tuning of the estimator parameters. Additional benefits would be the possibility of inclusion of outlier detection algorithms at the range or range-difference of arrival levels and better coping with loss of some of these measurements.

The main contribution of this paper is the design of a tightly coupled integrated navigation solution based on an LBL/USBL acoustic positioning system. In contrast with the solution proposed in Batista et al. (2011a), the range and RDOA are used directly in the observers feedback loop, hence avoiding intermediate computations, and no linearisations are carried out whatsoever. First, an attitude observer, that includes the estimation of rate gyro bias, is proposed, which is independent of the linear motion quantities. The proposed observer achieves GES error dynamics and it is computationally efficient. Topological limitations are avoided by relaxation of the constraints of the special orthogonal group, which are nevertheless verified asymptotically. Additional references are provided that yield estimates on $SO(3)$ based directly on the output of the proposed observer with meaningless additional computational burden. Afterwards, a position and linear velocity observer is proposed assuming exact angular data information, which also yields GES error dynamics. Finally, the cascade structure is analysed and it is shown that the error converges exponentially fast to zero for all initial conditions. This is, to the best of the authors' knowledge, the first contribution on the design of tightly coupled integrated LBL/USBL navigation system. Previous work by the authors can be found in Batista, Silvestre, and Oliveira (2013a) and Batista, Silvestre, and Oliveira (2013b), where the solutions for the estimation of the linear and angular motion quantities were presented independently. This paper improves those results by providing detailed proofs and by considering the

complete interconnected estimation structure, including its stability analysis.

The paper is organised as follows. The problem statement and the nominal system dynamics are introduced in Section 2. The problem of attitude estimation is considered, independently, in Section 3, while that of estimating the linear motion quantities is addressed in Section 4. The complete integrated navigation system is proposed and analysed in Section 5 and simulation results are presented in Section 6. Finally, Section 7 summarises the main conclusions and results of the paper.

1.1. Notation

Throughout the paper, the symbol $\mathbf{0}_{n\times m}$ denotes an $n\times m$ matrix of zeros, $\mathbf{I}_n$ an identity matrix with dimension $n\times n$, and $\text{diag}(\mathbf{A}_1,\ldots,\mathbf{A}_n)$ a block diagonal matrix. When the dimensions are omitted, the matrices are assumed of appropriate dimensions. For $\mathbf{x}\in\mathbb{R}^3$ and $\mathbf{y}\in\mathbb{R}^3$, $\mathbf{x}\times\mathbf{y}$ and $\mathbf{x}\cdot\mathbf{y}$ represent the cross and inner products, respectively. Finally, the Dirac delta function is denoted by $\delta(t)$.

2. Problem statement

Consider an underwater vehicle moving in a scenario where there is a set of fixed landmarks installed in an LBL configuration and suppose that the vehicle is equipped with a USBL acoustic positioning system, which measures not only the distance between the vehicle and each landmark but also the RDOA between the acoustic receivers of the USBL, from each landmark, as depicted in Figure 1. For further details on the USBL, please refer to Morgado et al. (2011), Morgado et al. (2010), and references therein. Further assume that the vehicle is equipped with a Doppler velocity log(DVL), which measures the velocity of the vehicle relative to the water, and a triad of orthogonally mounted rate gyros, which measures the angular velocity up to some offset. Finally, it is considered that the vehicle moves in the presence of a constant unknown ocean current. The problem considered in the paper is the design of a highly integrated tightly coupled estimation solution for the inertial position of the vehicle and its attitude, the ocean current velocity, and the rate gyro bias, with convergence guarantees.

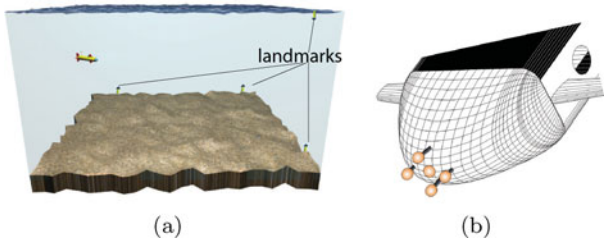

Figure 1. Mission scenario. (a) AUV and LBL array. (b) AUV with USBL array.

2.1. System dynamics

To set the problem framework, let $\{I\}$ denote a local inertial reference coordinate frame and $\{B\}$ a coordinate frame attached to the vehicle, usually called the body-fixed reference frame. The kinematics of the vehicle are described by

$$\begin{cases}\dot{\mathbf{p}}(t)=\mathbf{R}(t)\mathbf{v}(t)\\ \dot{\mathbf{R}}(t)=\mathbf{R}(t)\mathbf{S}(\boldsymbol{\omega}(t))\end{cases}, \tag{1}$$

where $\mathbf{p}(t)\in\mathbb{R}^3$ denotes the inertial position of the vehicle, $\mathbf{v}(t)\in\mathbb{R}^3$ is the velocity of the vehicle relative to $\{I\}$ and expressed in body-fixed coordinates, $\mathbf{R}(t)\in SO(3)$ is the rotation matrix from $\{B\}$ to $\{I\}$, $\boldsymbol{\omega}(t)\in\mathbb{R}^3$ is the angular velocity of $\{B\}$, expressed in body-fixed coordinates, and $\mathbf{S}(\boldsymbol{\omega})$ is the skew-symmetric matrix such that $\mathbf{S}(\boldsymbol{\omega})\boldsymbol{x}$ is the cross product $\boldsymbol{\omega}\times\boldsymbol{x}$.

The DVL provides the velocity of the vehicle relative to the water, expressed in body-fixed coordinates, denoted by $\mathbf{v}_r(t)\in\mathbb{R}^3$, such that

$$\mathbf{v}(t)=\mathbf{v}_r(t)+\mathbf{v}_c(t), \tag{2}$$

where $\mathbf{v}_c(t)\in\mathbb{R}^3$ is the ocean current velocity expressed in body-fixed coordinates, while the triad of rate gyros gives

$$\boldsymbol{\omega}_m(t)=\boldsymbol{\omega}(t)+\mathbf{b}_{\boldsymbol{\omega}}(t), \tag{3}$$

where $\mathbf{b}_{\boldsymbol{\omega}}(t)\in\mathbb{R}^3$ denotes the rate gyro bias, which is assumed constant, i.e.,

$$\dot{\mathbf{b}}_{\boldsymbol{\omega}}(t)=\mathbf{0}. \tag{4}$$

Let $\mathbf{s}_i\in\mathbb{R}^3$, $i=1,\ldots,N$, denote the inertial positions of the landmarks, and $\mathbf{a}_i\in\mathbb{R}^3$, $i=1,\ldots,M$, the positions of the array of receivers of the USBL relative to the origin of $\{B\}$, expressed in body-fixed coordinates. Then, the range measurement between the i-th landmark and the j-th acoustic receiver of the USBL is given by

$$r_{i,j}(t)=\|\mathbf{s}_i-\mathbf{p}(t)-\mathbf{R}(t)\mathbf{a}_j\|\in\mathbb{R}. \tag{5}$$

Define $\mathbf{u}(t):=\mathbf{R}(t)\mathbf{v}_r(t)$ and let ${}^I\mathbf{v}_c(t):=\mathbf{R}(t)\mathbf{v}_c(t)$ denote the ocean current velocity expressed in inertial coordinates. Assuming it is constant, and combining (1)–(5), yields the

nonlinear system

$$\begin{cases} \dot{\mathbf{p}}(t) = {}^{I}\mathbf{v}_c(t) + \mathbf{u}(t) \\ \dot{\mathbf{R}}(t) = \mathbf{R}(t)\mathbf{S}\left(\boldsymbol{\omega}_m(t) - \mathbf{b}_{\boldsymbol{\omega}}(t)\right) \\ {}^{I}\dot{\mathbf{v}}_c(t) = \mathbf{0}(t) \\ \dot{\mathbf{b}}_{\boldsymbol{\omega}}(t) = \mathbf{0} \\ r_{1,1}(t) = \|\mathbf{s}_1 - \mathbf{p}(t) - \mathbf{R}(t)\mathbf{a}_1\| \\ \vdots \\ r_{N,M}(t) = \|\mathbf{s}_N - \mathbf{p}(t) - \mathbf{R}(t)\mathbf{a}_M\| \end{cases}. \tag{6}$$

The problem considered in the paper is the design of an estimator for Equation (6) with global convergence guarantees.

2.2. *Long baseline/ultra short baseline configuration*

LBL acoustic configurations are one of the earliest methods employed for underwater navigation. These are characterised by the property that the distance between the transponders is long or similar to the distance between the vehicle and the transponders. This is in contrast with USBL systems, where the distance between the transponder and the vehicle is much larger than the distance between receivers of the USBL system. In common is the fact that, under standard assumptions, both the inertial position of the vehicle (for the LBL) and the position of the landmarks with respect to the vehicle, expressed in body-fixed coordinates, (for the USBL, in the so-called inverted configuration) are uniquely determined. This happens with the following standard assumptions, which are considered in the remainder of the paper.

Assumption 1: *The LBL acoustic positioning system includes at least four non-coplanar landmarks and the distance between the landmarks of the LBL is much larger than the distance between the receivers of the USBL acoustic positioning system.*

Assumption 2: *The USBL acoustic positioning system includes at least four non-coplanar receivers and the distance between the landmarks of the LBL is much larger than the distance between the receivers of the USBL acoustic positioning system.*

Remark 1: When there exist at least four noncoplanar landmarks (receivers), it is always possible to determine the inertial position of the vehicle (the position of the landmark with respect to the vehicle, expressed in body-fixed coordinates) from the range measurements from each landmark to the vehicle (from the range and RDOA between the landmark and the receivers of the array of the USBL). When there are fewer measurements that is not always possible and certain observability conditions must be met, see e.g. Batista, Silvestre, and Oliveira (2011b) for the case of single range measurements. The scope of this paper is on the combination of the USBL and the LBL measurements, taking full advantage of the large data set to improve performance and robustness to temporary sensor failure, while still guaranteeing convergence of the error to zero. As such, particular cases that do not satisfy Assumptions 2.1 and 2.2 are not treated, though it is rather straightforward to extrapolate the results presented herein to other cases considering the analysis that is detailed in Batista et al. (2011b).

3. Attitude and rate gyro bias estimation

This section details the design of an attitude observer that uses directly the ranges and RDOA and that achieves GES error dynamics. The proposed approach builds vaguely on two different methodologies previously proposed by the authors. First, a sensor-based observer for the rate gyro bias is developed by appropriate state definition, which bears some resemblance to the design proposed in Batista et al. (2011b), where the problems of source localisation and navigation based on single range measurements were addressed. Second, a cascade attitude observer is proposed assuming that the rate gyro bias is known. Finally, the overall cascade observer is proposed and its stability is analysed. The cascade design is similar, at large, to that proposed in Batista et al. (2012c). However, the structures of each individual observer are very different as they now rely on range and RDOA measurements instead of vector measurements.

3.1. *Rate gyro bias observer*

The dependence of the attitude observer (and, consequently, the bias observer) on the inertial position of the vehicle is highly undesirable and in fact it should not be required. Indeed, in an LBL/USBL framework, the positions of the LBL landmarks with respect to the vehicle, expressed in body-fixed coordinates, are indirectly available (after some computations). If one takes the difference between pairs of these vectors, one obtains a set of body-fixed vectors that correspond to constant known inertial vectors, obtained from the differences of the inertial positions of the LBL landmarks. As such, this information suffices to determine the attitude of the vehicle without the need of the inertial position of the vehicle. In fact, this is the idea of the approach proposed in Batista et al. (2011a). This section aims at achieving the same result but using directly the ranges and RDOA, hence achieving a tightly coupled structure.

Let $\mathcal{C}_{\mathbf{s}}$ denote a set of 2-combinations of elements of the set $\{1, \ldots, N\}$, e.g.

$$\mathcal{C}_{\mathbf{s}} = \{(1,2),(1,3),\ldots(1,N),(2,3),\ldots, (2,N),\ldots,(N-1,N)\},$$

and let $\mathcal{C}_{\mathbf{a}}$ denote a set of 2-combinations of elements of the set $\{1, \ldots, M\}$, e.g.

$$\mathcal{C}_{\mathbf{a}} = \{(1,2),(1,3),\ldots(1,M),(2,3),\ldots,(2,M),\ldots, (M-1,M)\}.$$

Define

$$q\left(m,n,i,j,t\right):=-\frac{1}{2}\left[r_{m,i}^{2}(t)-r_{n,i}^{2}(t)\right]+\frac{1}{2}\left[r_{m,j}^{2}(t)-r_{n,j}^{2}(t)\right] \tag{7}$$

for all $(m,n,i,j)\in\mathcal{C}_{\mathbf{s}}\times\mathcal{C}_{\mathbf{a}}$. First, notice that $q(m,n,i,j,t)$ is a direct function of the ranges and RDOA, as it is possible to rewrite it as

$$q\left(m,n,i,j,t\right)=\frac{1}{2}[r_{n,i}(t)+r_{n,j}(t)][r_{n,i}(t)-r_{n,j}(t)]-\frac{1}{2}[r_{m,i}(t)+r_{m,j}(t)][r_{m,i}(t)-r_{m,j}(t)].$$

Next, substituting Equation (5) in Equation (7) gives

$$q\left(m,n,i,j,t\right)=\left(\mathbf{s}_{m}-\mathbf{s}_{n}\right)^{T}\mathbf{R}(t)\left(\mathbf{a}_{i}-\mathbf{a}_{j}\right). \tag{8}$$

As it can be seen, the inertial position of the vehicle does not influence $q(m,n,i,j,t)$. Yet, it depends on the attitude of the vehicle and, considering all two-combinations of LBL landmarks and all two-combinations of USBL receivers, it is related to the entire geometric structure of the LBL/USBL positioning system. The idea of the bias observer is to use $q(m,n,i,j,t)$, for all $(m,n,i,j)\in\mathcal{C}_{\mathbf{s}}\times\mathcal{C}_{\mathbf{a}}$, as system states, which are measured, to estimate the rate gyro bias $\mathbf{b}_{\boldsymbol{\omega}}(t)$, which is unknown.

Before proceeding some additional definitions are required. In particular, define, for all $(i,j)\in\mathcal{C}_{\mathbf{a}}$, additional unit vectors $\mathbf{a}_{i,j}^{\perp_1}\in\mathbb{R}^3$ and $\mathbf{a}_{i,j}^{\perp_2}\in\mathbb{R}^3$ such that

$$\begin{cases}\frac{\mathbf{a}_i-\mathbf{a}_j}{\|\mathbf{a}_i-\mathbf{a}_j\|}\times\mathbf{a}_{i,j}^{\perp_1}=\mathbf{a}_{i,j}^{\perp_2}\\ \mathbf{a}_{i,j}^{\perp_1}\times\mathbf{a}_{i,j}^{\perp_2}=\frac{\mathbf{a}_i-\mathbf{a}_j}{\|\mathbf{a}_i-\mathbf{a}_j\|}\\ \mathbf{a}_{i,j}^{\perp_2}\times\frac{\mathbf{a}_i-\mathbf{a}_j}{\|\mathbf{a}_i-\mathbf{a}_j\|}=\mathbf{a}_{i,j}^{\perp_1}\end{cases}. \tag{9}$$

In short, the sets of vectors $\left\{\frac{\mathbf{a}_i-\mathbf{a}_j}{\|\mathbf{a}_i-\mathbf{a}_j\|},\mathbf{a}_{i,j}^{\perp_1},\mathbf{a}_{i,j}^{\perp_2}\right\}$, for all $(i,j)\in\mathcal{C}_{\mathbf{a}}$, form orthonormal bases of $\mathbb{R}^3$. Next, notice that under Assumption 2.2, it is always possible to express all additional vectors $\mathbf{a}_{i,j}^{\perp_1}$ and $\mathbf{a}_{i,j}^{\perp_2}$ as a linear combination of vectors $\mathbf{a}_k-\mathbf{a}_l$. Let these be defined as

$$\begin{cases}\mathbf{a}_{i,j}^{\perp_1}=\sum\limits_{(k,l)\in\mathcal{C}_{\mathbf{a}}}\phi_1\left(i,j,k,l\right)\left(\mathbf{a}_k-\mathbf{a}_l\right)\\ \mathbf{a}_{i,j}^{\perp_2}=\sum\limits_{(k,l)\in\mathcal{C}_{\mathbf{a}}}\phi_2\left(i,j,k,l\right)\left(\mathbf{a}_k-\mathbf{a}_l\right)\end{cases} \tag{10}$$

for all $(i,j)\in\mathcal{C}_{\mathbf{a}}$, where $\phi_1\left(i,j,k,l\right),\phi_2\left(i,j,k,l\right)\in\mathbb{R}$ are the linear combination coefficients.

The nominal system dynamics of the rate gyro bias observer are now derived. Taking the derivative of Equation (8), and using Equation (6), gives

$$\dot{q}\left(m,n,i,j,t\right)=\left(\mathbf{s}_{m}-\mathbf{s}_{n}\right)^{T}\mathbf{R}(t)\mathbf{S}\left(\boldsymbol{\omega}_{m}(t)\right)\left(\mathbf{a}_{i}-\mathbf{a}_{j}\right)-\left(\mathbf{s}_{m}-\mathbf{s}_{n}\right)^{T}\mathbf{R}(t)\mathbf{S}(\mathbf{b}_{\boldsymbol{\omega}}(t))(\mathbf{a}_{i}-\mathbf{a}_{j}). \tag{11}$$

Express $\boldsymbol{\omega}_m(t)$ as the linear combination

$$\boldsymbol{\omega}_{m}(t)=\boldsymbol{\omega}_{m}(t)\cdot\frac{\left(\mathbf{a}_{i}-\mathbf{a}_{j}\right)}{\|\left(\mathbf{a}_{i}-\mathbf{a}_{j}\right)\|}\frac{\left(\mathbf{a}_{i}-\mathbf{a}_{j}\right)}{\|\left(\mathbf{a}_{i}-\mathbf{a}_{j}\right)\|}+\boldsymbol{\omega}_{m}(t)\cdot\mathbf{a}_{i,j}^{\perp_1}\mathbf{a}_{i,j}^{\perp_1}+\boldsymbol{\omega}_{m}(t)\cdot\mathbf{a}_{i,j}^{\perp_2}\mathbf{a}_{i,j}^{\perp_2}. \tag{12}$$

Using Equation (12) first and then Equation (9), it is possible to write

$$\begin{aligned}\boldsymbol{\omega}_{m}(t)\times\left(\mathbf{a}_{i}-\mathbf{a}_{j}\right)&=\boldsymbol{\omega}_{m}(t)\cdot\mathbf{a}_{i,j}^{\perp_1}\left[\mathbf{a}_{i,j}^{\perp_1}\times\left(\mathbf{a}_{i}-\mathbf{a}_{j}\right)\right]\\&\quad+\boldsymbol{\omega}_{m}(t)\cdot\mathbf{a}_{i,j}^{\perp_2}\left[\mathbf{a}_{i,j}^{\perp_2}\times\left(\mathbf{a}_{i}-\mathbf{a}_{j}\right)\right]\\&=\boldsymbol{\omega}_{m}(t)\cdot\mathbf{a}_{i,j}^{\perp_2}\|\mathbf{a}_{i}-\mathbf{a}_{j}\|\mathbf{a}_{i,j}^{\perp_1}\\&\quad-\boldsymbol{\omega}_{m}(t)\cdot\mathbf{a}_{i,j}^{\perp_1}\|\mathbf{a}_{i}-\mathbf{a}_{j}\|\mathbf{a}_{i,j}^{\perp_2}.\end{aligned} \tag{13}$$

Substituting Equation (10) in Equation (13) gives

$$\begin{aligned}&\boldsymbol{\omega}_{m}(t)\times\left(\mathbf{a}_{i}-\mathbf{a}_{j}\right)\\&=\boldsymbol{\omega}_{m}(t)\cdot\mathbf{a}_{i,j}^{\perp_2}\|\mathbf{a}_{i}-\mathbf{a}_{j}\|\sum_{(k,l)\in\mathcal{C}_{\mathbf{a}}}\phi_1\left(i,j,k,l\right)\left(\mathbf{a}_{k}-\mathbf{a}_{l}\right)\\&\quad-\boldsymbol{\omega}_{m}(t)\cdot\mathbf{a}_{i,j}^{\perp_1}\|\mathbf{a}_{i}-\mathbf{a}_{j}\|\sum_{(k,l)\in\mathcal{C}_{\mathbf{a}}}\phi_2\left(i,j,k,l\right)\left(\mathbf{a}_{k}-\mathbf{a}_{l}\right).\end{aligned} \tag{14}$$

Substituting Equation (14) in the first term of the right side of Equation (11), and using Equation (8), gives

$$\begin{aligned}&\left(\mathbf{s}_{m}-\mathbf{s}_{n}\right)^{T}\mathbf{R}(t)\mathbf{S}\left(\boldsymbol{\omega}_{m}(t)\right)\left(\mathbf{a}_{i}-\mathbf{a}_{j}\right)\\&=\boldsymbol{\omega}_{m}(t)\cdot\mathbf{a}_{i,j}^{\perp_2}\|\mathbf{a}_{i}-\mathbf{a}_{j}\|\sum_{(k,l)\in\mathcal{C}_{\mathbf{a}}}\phi_1\left(i,j,k,l\right)q\left(m,n,k,l,t\right)\\&\quad-\boldsymbol{\omega}_{m}(t)\cdot\mathbf{a}_{i,j}^{\perp_1}\|\mathbf{a}_{i}-\mathbf{a}_{j}\|\sum_{(k,l)\in\mathcal{C}_{\mathbf{a}}}\phi_2\left(i,j,k,l\right)q\left(m,n,k,l,t\right).\end{aligned} \tag{15}$$

Following the same circle of ideas, it is possible to rewrite the second term of the right side of Equation (11) as

$$\begin{aligned}&\left(\mathbf{s}_{m}-\mathbf{s}_{n}\right)^{T}\mathbf{R}(t)\mathbf{S}\left(\mathbf{b}_{\boldsymbol{\omega}}(t)\right)\left(\mathbf{a}_{i}-\mathbf{a}_{j}\right)\\&=\mathbf{b}_{\boldsymbol{\omega}}(t)\cdot\mathbf{a}_{i,j}^{\perp_2}\|\mathbf{a}_{i}-\mathbf{a}_{j}\|\sum_{(k,l)\in\mathcal{C}_{\mathbf{a}}}\phi_1\left(i,j,k,l\right)q\left(m,n,k,l,t\right)\\&\quad-\mathbf{b}_{\boldsymbol{\omega}}(t)\cdot\mathbf{a}_{i,j}^{\perp_1}\|\mathbf{a}_{i}-\mathbf{a}_{j}\|\sum_{(k,l)\in\mathcal{C}_{\mathbf{a}}}\phi_2\left(i,j,k,l\right)q\left(m,n,k,l,t\right).\end{aligned} \tag{16}$$

Substituting Equations (15) and (16) in Equation (11) gives the nonlinear dynamics

$$\begin{aligned}
&\dot{q}\,(m,n,i,j,t)\\
&=\boldsymbol{\omega}_m(t)\cdot\mathbf{a}_{i,j}^{\perp_2}\|\mathbf{a}_i-\mathbf{a}_j\|\sum_{(k,l)\in\mathcal{C}_\mathbf{a}}\phi_1(i,j,k,l)\,q(m,n,k,l,t)\\
&\quad-\boldsymbol{\omega}_m(t)\cdot\mathbf{a}_{i,j}^{\perp_1}\|\mathbf{a}_i-\mathbf{a}_j\|\sum_{(k,l)\in\mathcal{C}_\mathbf{a}}\phi_2(i,j,k,l)\,q(m,n,k,l,t)\\
&\quad+\mathbf{b}_{\boldsymbol{\omega}}(t)\cdot\mathbf{a}_{i,j}^{\perp_1}\|\mathbf{a}_i-\mathbf{a}_j\|\sum_{(k,l)\in\mathcal{C}_\mathbf{a}}\phi_2(i,j,k,l)\,q(m,n,k,l,t)\\
&\quad-\mathbf{b}_{\boldsymbol{\omega}}(t)\cdot\mathbf{a}_{i,j}^{\perp_2}\|\mathbf{a}_i-\mathbf{a}_j\|\sum_{(k,l)\in\mathcal{C}_\mathbf{a}}\phi_1(i,j,k,l)\,q(m,n,k,l,t)
\end{aligned}\tag{17}$$

for all $(m,n,i,j)\in\mathcal{C}_\mathbf{s}\times\mathcal{C}_\mathbf{a}$. Notice that Equation (17) depends only on the USBL array geometry, the rate gyro measurements $\boldsymbol{\omega}_m(t)$, the additional quantities $q(m,n,i,j,t)$, the linear coefficients $\phi_1(i,j,k,l)$ and $\phi_2(i,j,k,l)$, all available, and the unknown rate gyro bias $\mathbf{b}_{\boldsymbol{\omega}}(t)$.

Consider the rate gyro bias observer dynamics given by

$$\begin{aligned}
&\dot{\hat{q}}\,(m,n,i,j,t)\\
&=\boldsymbol{\omega}_m(t)\cdot\mathbf{a}_{i,j}^{\perp_2}\|\mathbf{a}_i-\mathbf{a}_j\|\sum_{(k,l)\in\mathcal{C}_\mathbf{a}}\phi_1(i,j,k,l)\,\hat{q}\,(m,n,k,l,t)\\
&\quad-\boldsymbol{\omega}_m(t)\cdot\mathbf{a}_{i,j}^{\perp_1}\|\mathbf{a}_i-\mathbf{a}_j\|\sum_{(k,l)\in\mathcal{C}_\mathbf{a}}\phi_2(i,j,k,l)\,\hat{q}\,(m,n,k,l,t)\\
&\quad+\hat{\mathbf{b}}_{\boldsymbol{\omega}}(t)\cdot\mathbf{a}_{i,j}^{\perp_1}\|\mathbf{a}_i-\mathbf{a}_j\|\sum_{(k,l)\in\mathcal{C}_\mathbf{a}}\phi_2(i,j,k,l)\,q(m,n,k,l,t)\\
&\quad-\hat{\mathbf{b}}_{\boldsymbol{\omega}}(t)\cdot\mathbf{a}_{i,j}^{\perp_2}\|\mathbf{a}_i-\mathbf{a}_j\|\sum_{(k,l)\in\mathcal{C}_\mathbf{a}}\phi_1(i,j,k,l)\,q(m,n,k,l,t)\\
&\quad+\alpha(m,n,i,j)\,[q(m,n,i,j,t)-\hat{q}\,(m,n,i,j,t)]
\end{aligned}\tag{18}$$

for all $(m,n,i,j)\in\mathcal{C}_\mathbf{s}\times\mathcal{C}_\mathbf{a}$, and

$$\begin{aligned}
\dot{\hat{\mathbf{b}}}_{\boldsymbol{\omega}}(t)=&\sum_{(m,n,i,j)\in\mathcal{C}_\mathbf{s}\times\mathcal{C}_\mathbf{a}}\beta(m,n,i,j)\,\|\mathbf{a}_i-\mathbf{a}_j\|\\
&[q(m,n,i,j,t)-\hat{q}\,(m,n,i,j,t)]\\
&\left[\mathbf{a}_{i,j}^{\perp_1}\sum_{(k,l)\in\mathcal{C}_\mathbf{a}}\phi_2(i,j,k,l)\,q(m,n,k,l,t)\right.\\
&\left.-\mathbf{a}_{i,j}^{\perp_2}\sum_{(k,l)\in\mathcal{C}_\mathbf{a}}\phi_1(i,j,k,l)\,q(m,n,k,l,t)\right],
\end{aligned}\tag{19}$$

where $\alpha(m,n,i,j)>0$ and $\beta(m,n,i,j)>0$, for all $(m,n,i,j)\in\mathcal{C}_\mathbf{s}\times\mathcal{C}_\mathbf{a}$, are observer tuning parameters.

Let $\tilde{q}\,(m,n,i,j,t):=q\,(m,n,i,j,t)-\hat{q}(m,n,i,j,t)$, for all $(m,n,i,j)\in\mathcal{C}_\mathbf{s}\times\mathcal{C}_\mathbf{a}$ and $\tilde{\mathbf{b}}_{\boldsymbol{\omega}}(t):=\mathbf{b}_{\boldsymbol{\omega}}(t)-\hat{\mathbf{b}}_{\boldsymbol{\omega}}(t)$ denote the observer error. Then, the observer error dynamics are given by

$$\begin{aligned}
&\dot{\tilde{q}}\,(m,n,i,j,t)\\
&=\boldsymbol{\omega}_m(t)\cdot\mathbf{a}_{i,j}^{\perp_2}\|\mathbf{a}_i-\mathbf{a}_j\|\sum_{(k,l)\in\mathcal{C}_\mathbf{a}}\phi_1(i,j,k,l)\,\tilde{q}\,(m,n,k,l,t)\\
&\quad-\boldsymbol{\omega}_m(t)\cdot\mathbf{a}_{i,j}^{\perp_1}\|\mathbf{a}_i-\mathbf{a}_j\|\sum_{(k,l)\in\mathcal{C}_\mathbf{a}}\phi_2(i,j,k,l)\,\tilde{q}\,(m,n,k,l,t)\\
&\quad+\tilde{\mathbf{b}}_{\boldsymbol{\omega}}(t)\cdot\mathbf{a}_{i,j}^{\perp_1}\|\mathbf{a}_i-\mathbf{a}_j\|\sum_{(k,l)\in\mathcal{C}_\mathbf{a}}\phi_2(i,j,k,l)\,q(m,n,k,l,t)\\
&\quad-\tilde{\mathbf{b}}_{\boldsymbol{\omega}}(t)\cdot\mathbf{a}_{i,j}^{\perp_2}\|\mathbf{a}_i-\mathbf{a}_j\|\sum_{(k,l)\in\mathcal{C}_\mathbf{a}}\phi_1(i,j,k,l)\,q(m,n,k,l,t)\\
&\quad-\alpha(m,n,i,j)\,\tilde{q}\,(m,n,i,j,t)
\end{aligned}$$

for all $(m,n,i,j)\in\mathcal{C}_\mathbf{s}\times\mathcal{C}_\mathbf{a}$, and

$$\begin{aligned}
\dot{\tilde{\mathbf{b}}}_{\boldsymbol{\omega}}(t)=&-\sum_{(m,n,i,j)\in\mathcal{C}_\mathbf{s}\times\mathcal{C}_\mathbf{a}}\beta(m,n,i,j)\,\tilde{q}\,(m,n,i,j,t)\\
&\|\mathbf{a}_i-\mathbf{a}_j\|\left[\mathbf{a}_{i,j}^{\perp_1}\sum_{(k,l)\in\mathcal{C}_\mathbf{a}}\phi_2(i,j,k,l)\right.\\
&q\,(m,n,k,l,t)-\mathbf{a}_{i,j}^{\perp_2}\sum_{(k,l)\in\mathcal{C}_\mathbf{a}}\phi_1(i,j,k,l)\\
&\left.q\,(m,n,k,l,t)\right].
\end{aligned}$$

The following theorem establishes that the resulting rate gyro bias observer has GES error dynamics.

Theorem 3.1: *Suppose that Assumptions 1 and 2 are satisfied and consider the rate gyro bias observer given by Equations*(18) *and* (19)*, where* $\alpha(m,n,i,j)>0$ *and* $\beta(m,n,i,j)>0$ *for all* $(m,n,i,j)\in\mathcal{C}_\mathbf{s}\times\mathcal{C}_\mathbf{a}$*. Then, the origin of the error dynamics is a GES equilibrium point.*

Proof: Let $\tilde{\boldsymbol{x}}_1(t):=[\ldots\,\tilde{q}\,(m,n,i,j,t)\ldots\,\tilde{\mathbf{b}}_{\boldsymbol{\omega}}^T(t)\,]^T\in\mathbb{R}^{{}_2^NC\,{}_2^MC+3}$,$(m,n,i,j)\in\mathcal{C}_\mathbf{s}\times\mathcal{C}_\mathbf{a}$, denote the estimator error, in compact form, where ${}_2^NC=N(N-1)/2$ and ${}_2^MC=M(M-1)/2$ denote the number of two-combinations of N and M elements, respectively. Define

$$\begin{aligned}
V_1(\tilde{\boldsymbol{x}}_1(t)):=&\frac{1}{2}\sum_{(i,j,k,l)\in\mathcal{C}_\mathbf{s}\times\mathcal{C}_\mathbf{a}}\beta(m,n,i,j)\,[\tilde{q}\,(m,n,i,j,t)]^2\\
&+\frac{1}{2}\|\tilde{\mathbf{b}}_{\boldsymbol{\omega}}(t)\|^2
\end{aligned}$$

as a Lyapunov function candidate. Clearly,

$$\gamma_1\,\|\tilde{\boldsymbol{x}}_1(t)\|^2\le V_1(\tilde{\boldsymbol{x}}_1(t))\le\gamma_2\,\|\tilde{\boldsymbol{x}}_1(t)\|^2,\tag{20}$$

where

$$\gamma_1:=\frac{1}{2}\min(1,\beta(m,n,i,j)),\,(m,n,i,j)\in\mathcal{C}_\mathbf{s}\times\mathcal{C}_\mathbf{a}$$

and

$$\gamma_2 := \frac{1}{2}\max\left(1, \beta\left(m, n, i, j\right)\right), (m, n, i, j) \in \mathcal{C}_{\mathbf{s}} \times \mathcal{C}_{\mathbf{a}}.$$

The time derivative of $V_1\left(\tilde{\boldsymbol{x}}_1(t)\right)$ can be written, after some computations, as

$$\begin{aligned}\dot{V}_1\left(\tilde{\boldsymbol{x}}_1(t)\right) &= -\tilde{\boldsymbol{x}}_1^T(t)\mathbf{C}_1^T\mathbf{C}_1\tilde{\boldsymbol{x}}_1(t)\\ &= -\sum_{(i,j,k,l)\in\mathcal{C}_{\mathbf{s}}\times\mathcal{C}_{\mathbf{a}}} \alpha\left(m, n, i, j\right)\beta\left(m, n, i, j\right)\\ &\quad \left[\tilde{q}\left(m, n, i, j, t\right)\right]^2,\end{aligned}$$

where $\mathbf{C}_1 = [\,\mathrm{diag}(\sqrt{\alpha(m,\,n,\,i,\,j)\beta(m,\,n,\,i,\,j)})\;\mathbf{0}\,]$. Hence,

$$\dot{V}_1\left(\tilde{\boldsymbol{x}}_1(t)\right) \leq 0. \tag{21}$$

Now, notice that the error dynamics can be written as the linear time-varying (LTV) system

$$\dot{\tilde{\boldsymbol{x}}}_1(t) = \boldsymbol{\mathcal{A}}_1(t)\tilde{\boldsymbol{x}}_1(t), \tag{22}$$

where

$$\boldsymbol{\mathcal{A}}_1(t) = \begin{bmatrix}\boldsymbol{\mathcal{A}}_{11}(t) & \boldsymbol{\mathcal{A}}_{12}(t)\\ \boldsymbol{\mathcal{A}}_{21}(t) & \mathbf{0}\end{bmatrix}$$

and each row of the matrix $\boldsymbol{\mathcal{A}}_{12}(t)$, corresponding to the state error $\tilde{q}\left(m, n, i, j, t\right)$, is given by

$$\begin{aligned}&\|\mathbf{a}_i - \mathbf{a}_j\| \sum_{(k,l)\in\mathcal{C}_{\mathbf{a}}} \phi_2\left(i, j, k, l\right) q\left(m, n, k, l, t\right)\left(\mathbf{a}_{i,j}^{\perp_1}\right)^T\\ &-\|\mathbf{a}_i - \mathbf{a}_j\| \sum_{(k,l)\in\mathcal{C}_{\mathbf{a}}} \phi_1\left(i, j, k, l\right) q\left(m, n, k, l, t\right)\left(\mathbf{a}_{i,j}^{\perp_2}\right)^T.\end{aligned}$$

The definitions of $\boldsymbol{\mathcal{A}}_{11}(t)$ and $\boldsymbol{\mathcal{A}}_{21}(t)$ are omitted as they are not required in the sequel. If in addition to Equations (20) and (21), the pair $(\boldsymbol{\mathcal{A}}_1(t), \mathbf{C}_1)$ is uniformly completely observable, then the origin of the LTV system (22) is a GES equilibrium point, see Khalil (2001, Example 8.11). The remainder of the proof amounts to show that the pair $(\boldsymbol{\mathcal{A}}_1(t), \mathbf{C}_1)$ is uniformly completely observable. For any piecewise continuous, bounded matrix $\mathbf{K}_1(t)$, of compatible dimensions, uniform complete observability of the pair $(\boldsymbol{\mathcal{A}}_1(t), \mathbf{C}_1)$ is equivalent to uniform complete observability of the pair $(\mathbf{A}_1(t), \mathbf{C}_1)$, with $\mathbf{A}_1(t) := \boldsymbol{\mathcal{A}}_1(t) - \mathbf{K}_1(t)\mathbf{C}_1$, see Ioannou and Sun (1995, Lemma 4.8.1). Now, notice that, attending to the particular forms of $\mathbf{C}_1$ and $\boldsymbol{\mathcal{A}}_1(t)$, there exists a continuous bounded matrix $\mathbf{K}_1(t)$, which depends explicitly on the observer parameters, the rate gyro readings, $\boldsymbol{\omega}_m(t)$, the USBL structure, the linear coefficients $\phi_1(i, j, k, l)$ and $\phi_2(i, j, k, l)$, and $q(m, n, i, j, t)$, $(m, n, i, j) \in \mathcal{C}_{\mathbf{s}} \times \mathcal{C}_{\mathbf{a}}$, such that

$$\mathbf{A}_1(t) = \begin{bmatrix}\mathbf{0} & \boldsymbol{\mathcal{A}}_{12}(t)\\ \mathbf{0} & \mathbf{0}\end{bmatrix}.$$

The expression of $\mathbf{K}_1(t)$ is not presented here as it is evident from the context and it is not required in the sequel. It remains to show that the pair $(\mathbf{A}_1(t), \mathbf{C}_1)$ is uniformly completely observable, i.e., that there exist positive constants ϵ_1, ϵ_2, and δ such that

$$\epsilon_1\mathbf{I} \preceq \boldsymbol{\mathcal{W}}_1\left(t, t+\delta\right) \preceq \epsilon_2\mathbf{I} \tag{23}$$

for all $t \geq t_0$, where $\boldsymbol{\mathcal{W}}_1\left(t_0, t_f\right)$ is the observability Gramian associated with the pair $(\mathbf{A}_1(t), \mathbf{C}_1)$ on $[t_0, t_f]$. Since the entries of both $\mathbf{A}_1(t)$ and $\mathbf{C}_1$ are continuous and bounded, the right side of Equation (23) is evidently verified. Therefore, only the left side of Equation (23) requires verification. Let

$$\begin{aligned}\mathbf{d} = \left[\,\ldots\, d_{m,n,i,j}\, \ldots\, \mathbf{d}_2^T\,\right]^T &\in \mathbb{R}_2^{N C_2^M C+3},\\ d_{m,n,i,j} \in \mathbb{R},\ (m, n, i, j) &\in \mathcal{C}_{\mathbf{s}} \times \mathcal{C}_{\mathbf{a}},\ \mathbf{d}_2 \in \mathbb{R}^3\end{aligned}$$

be a unit vector and define

$$\begin{aligned}\mathbf{f}\left(\tau, t\right) := [\,\ldots\, f_{m,n,i,j}\left(\tau, t\right)\ldots]^T &\in \mathbb{R}_2^{N C_2^M C},\\ (m, n, i, j) &\in \mathcal{C}_{\mathbf{s}} \times \mathcal{C}_{\mathbf{a}},\end{aligned}$$

where

$$\begin{aligned}f_{m,n,i,j}\left(\tau, t\right) := &\sqrt{\alpha\left(m, n, i, j\right)\beta\left(m, n, i, j\right)}\\ &\left(d_{m,n,i,j} + \int_t^\tau \|\mathbf{a}_i - \mathbf{a}_j\|\right.\\ &\sum_{(k,l)\in\mathcal{C}_{\mathbf{a}}} \phi_2\left(i, j, k, l\right) q\left(m, n, k, l, \sigma\right)\mathbf{a}_{i,j}^{\perp_1}\\ &\cdot \mathbf{d}_2 d\sigma - \int_t^\tau \|\mathbf{a}_i - \mathbf{a}_j\| \sum_{(k,l)\in\mathcal{C}_{\mathbf{a}}} \phi_1\left(i, j, k, l\right)\\ &\left. q\left(m, n, k, l, \sigma\right)\mathbf{a}_{i,j}^{\perp_2} \cdot \mathbf{d}_2 d\sigma\right),\end{aligned} \tag{24}$$

$\tau \in [t, t+\delta]$, $t \geq t_0$. It is easy to show that

$$\mathbf{d}^T\boldsymbol{\mathcal{W}}_1\left(t, t+\delta\right)\mathbf{d} = \int_t^{t+\delta} \|\mathbf{f}\left(\tau, t\right)\|^2 d\tau.$$

Reversing the train of thought used to obtain Equation (15) but considering $\mathbf{d}_2$ instead of $\boldsymbol{\omega}_m(t)$, i.e., substituting Equation (8) in Equation (24), and then using Equations (10) and (9), it is possible to rewrite $f_{m,n,i,j}(\tau, t)$ as

$$\begin{aligned}f_{m,n,i,j}\left(\tau, t\right) := &\sqrt{\alpha\left(m, n, i, j\right)\beta\left(m, n, i, j\right)}\\ &\left(d_{m,n,i,j} - \int_t^\tau \left(\mathbf{s}_m - \mathbf{s}_n\right)^T\mathbf{R}(\sigma)\mathbf{S}\left(\mathbf{d}_2\right)\left(\mathbf{a}_i - \mathbf{a}_j\right)d\sigma\right).\end{aligned}$$

The derivative of $f_{m,\,n,\,i,\,j}(\tau, t)$ with respect to τ is given by

$$\frac{\partial}{\partial \tau} f_{m,n,i,j}(\tau, t) := -\sqrt{\alpha(m, n, i, j)\,\beta(m, n, i, j)}\,(\mathbf{s}_m - \mathbf{s}_n)^T\,\mathbf{R}(t)\mathbf{S}(\mathbf{d}_2)(\mathbf{a}_i - \mathbf{a}_j).$$

Under Assumptions 2.1 and 2.2, one can conclude that there exists a positive constant μ such that $\left\|\frac{\partial}{\partial \tau}\mathbf{f}(t, t)\right\| > \mu\,\|\mathbf{d}_2\|$ for all non-null vectors $\mathbf{d}_2$ and $t \geq t_0$. Fix $\delta > 0$. Resorting to Batista et al. (2011b, Proposition 2), it follows that there exists $\nu_1 > 0$ such that

$$\left\|\int_t^{t+\delta} \frac{\partial}{\partial \tau}\mathbf{f}(\sigma, t)\,d\sigma\right\| > \nu_1\,\|\mathbf{d}_2\|$$

for all non-null vectors $\mathbf{d}_2$ and $t \geq t_0$. Fix $\epsilon > 0$ sufficiently small such that

$$|d_{m,n,i,j}| < \epsilon \tag{25}$$

for all $(m, n, i, j) \in \mathcal{C}_\mathbf{s} \times \mathcal{C}_\mathbf{a}$ and

$$\epsilon < \frac{1}{2}\nu_1\,\|\mathbf{d}_2\|.$$

Notice that this is always possible as the smallest ϵ is the largest $\|\mathbf{d}_2\|$ is, as $\mathbf{d}$ is a unit vector. Then, it is clear that there exists ν_2 such that $\|\mathbf{f}(t + \delta, t)\| \geq \nu_2$ for all $t \geq t_0$ and all unit vectors $\mathbf{d}$ that satisfy Equation (25). Resorting to Batista et al. (2011b, Proposition 2) again, it follows that there exists $\nu_3 > 0$ such that, for all unit vectors $\mathbf{d}$ that satisfy Equation (25), (23) holds for all $t \geq t_0$, with $\epsilon_1 = \nu_3$. Suppose now that there exists $d_{m,\,n,\,i,\,j}$ such that

$$|d_{m,n,i,j}| \geq \epsilon. \tag{26}$$

In that case, it is possible to see that $\|\mathbf{f}(t, t)\| \geq \epsilon$ for all $t \geq t_0$. Hence, resorting to Batista et al. (2011b, Proposition 2) again, it follows that there exists $\nu_4 > 0$ such that, for all unit vectors $\mathbf{d}$ that satisfy Equation (26) for some $(m, n, i, j) \in \mathcal{C}_\mathbf{s} \times \mathcal{C}_\mathbf{a}$, Equation (23) holds for all $t \geq t_0$, with $\epsilon_1 = \nu_4$. But then it follows that Equation (23) holds for all $t \geq t_0$ and unit vectors $\mathbf{d}$, with $\epsilon_1 := \min(\nu_3, \nu_4)$, which means that the pair $(\mathbf{A}_1(t), \mathbf{C}_1)$ is uniformly completely observable, hence concluding the proof. □

3.2. *Attitude observer*

Let

$$\boldsymbol{x}_2(t) := \left[\mathbf{z}_1^T(t)\ \mathbf{z}_2^T(t)\ \mathbf{z}_3^T(t)\right]^T \in \mathbb{R}^9$$

be a column representation of $\mathbf{R}(t)$, where

$$\mathbf{R}(t) = \begin{bmatrix} \mathbf{z}_1^T(t) \\ \mathbf{z}_2^T(t) \\ \mathbf{z}_3^T(t) \end{bmatrix},$$

with $\mathbf{z}_i(t) \in \mathbb{R}^3$, $i = 1, 2, 3$. Then, it is easy to show that $\dot{\boldsymbol{x}}_2(t) = -\mathbf{S}_3(\boldsymbol{\omega}_m(t) - \mathbf{b}_\omega(t))\,\boldsymbol{x}_2(t)$, where $\mathbf{S}_3(\mathbf{x}) := \mathrm{diag}(\mathbf{S}(\mathbf{x}), \mathbf{S}(\mathbf{x}), \mathbf{S}(\mathbf{x})) \in \mathbb{R}^{9\times 9}$.

From Equation (8), it is possible to write $q(m, n, i, j, t)$ as a linear combination of elements of $\boldsymbol{x}_2(t)$, i.e., $q(m, n, i, j, t) = \mathbf{c}_{m,n,i,j} \cdot \boldsymbol{x}_2(t)$, where

$$\mathbf{c}_{m,n,i,j} := \begin{bmatrix} (\mathbf{a}_i - \mathbf{a}_j) & \mathbf{0} & \mathbf{0} \\ \mathbf{0} & (\mathbf{a}_i - \mathbf{a}_j) & \mathbf{0} \\ \mathbf{0} & \mathbf{0} & (\mathbf{a}_i - \mathbf{a}_j) \end{bmatrix} (\mathbf{s}_m - \mathbf{s}_n) \in \mathbb{R}^9.$$

Let $\mathbf{q}(t) := [\ldots\, q(m, n, i, j, t)\, \ldots]^T \in \mathbb{R}^{M C_2^M C}$, $(m, n, i, j) \in \mathcal{C}_\mathbf{s} \times \mathcal{C}_\mathbf{a}$. Then, it is possible to write $\mathbf{q}(t) = \mathbf{C}_2\boldsymbol{x}_2(t)$, where $\mathbf{C}_2 \in \mathbb{R}^{N C_2^M C \times 9}$ is omitted as it is evident from the context. Under Assumptions 2.1 and 2.2 it is possible to show that $\mathbf{C}_2$ has full rank.

Consider the attitude observer given by

$$\dot{\hat{\boldsymbol{x}}}_2(t) = -\mathbf{S}_3(\boldsymbol{\omega}_m(t) - \mathbf{b}_\omega(t))\,\hat{\boldsymbol{x}}_2(t) + \mathbf{C}_2^T\mathbf{Q}^{-1}\left[\mathbf{q}(t) - \mathbf{C}_2\hat{\boldsymbol{x}}_2(t)\right], \tag{27}$$

where $\mathbf{Q} = \mathbf{Q}^T \in \mathbb{R}^{N C_2^M C \times N C_2^M C}$ is a positive definite matrix, and define the error variable $\tilde{\boldsymbol{x}}_2(t) = \boldsymbol{x}_2(t) - \hat{\boldsymbol{x}}_2(t)$. Then, the observer error dynamics are given by

$$\dot{\tilde{\boldsymbol{x}}}_2(t) = \boldsymbol{\mathcal{A}}_2(t)\tilde{\boldsymbol{x}}_2(t), \tag{28}$$

where $\boldsymbol{\mathcal{A}}_2(t) := -[\mathbf{S}_3(\boldsymbol{\omega}_m(t) - \mathbf{b}_\omega(t)) + \mathbf{C}_2^T\mathbf{Q}^{-1}\mathbf{C}_2]$.

The following theorem is the main result of this section.

Theorem 3.2: *Suppose that the rate gyro bias is known and consider the attitude observer* (27)*, where* $\boldsymbol{Q}\succ\mathbf{0}$ *is a design parameter. Then, under Assumptions* 2.1 *and* 2.2*, the origin of the observer error dynamics* (28) *is a GES equilibrium point.*

Proof: The proof follows by considering the Lyapunov candidate function

$$V_2(\tilde{\boldsymbol{x}}_2(t)) := \frac{1}{2}\,\|\tilde{\boldsymbol{x}}_2(t)\|^2.$$

It is similar to that of Batista et al. (2012c, Theorem 2) and therefore it is omitted. The only difference is, in fact, in the definition of $\mathbf{C}_2$, which is nevertheless full rank, the only requirement for the proof. □

3.3. Cascade observer

This section presents the overall cascade observer and its stability analysis. In Section 3.1, an observer was derived, based directly on the ranges and RDOA, that provides an estimate of the bias, with GES dynamics. The idea of the cascade observer is to feed the attitude observer proposed in Section 3.2 with the bias estimate provided by the bias observer proposed in Section 3.1. The bias observer remains the same, given by Equations (18) and (19), whereas the attitude observer is now written as

$$\begin{aligned}\dot{\hat{\boldsymbol{x}}}_2(t) = &-\mathbf{S}_3(\boldsymbol{\omega}_m(t) - \hat{\mathbf{b}}_{\boldsymbol{\omega}}(t))\hat{\boldsymbol{x}}_2(t) \\ &+ \mathbf{C}_2^T \mathbf{Q}^{-1}\left[\mathbf{q}(t) - \mathbf{C}_2\hat{\boldsymbol{x}}_2(t)\right].\end{aligned} \tag{29}$$

The error dynamics corresponding to the bias observer are the same and, therefore, Theorem 3.1 applies. Evidently, the use of an estimate of the bias instead of the bias itself in the attitude observer introduces an error, and the stability of the system must be further examined. In this situation, the error dynamics of the cascade observer can be written as

$$\begin{cases}\dot{\tilde{\boldsymbol{x}}}_1(t) = \boldsymbol{\mathcal{A}}_1(t)\tilde{\boldsymbol{x}}_1(t) \\ \dot{\tilde{\boldsymbol{x}}}_2(t) = [\boldsymbol{\mathcal{A}}_2(t) - \mathbf{S}_3\left(\tilde{\mathbf{b}}_{\boldsymbol{\omega}}(t)\right)]\tilde{\boldsymbol{x}}_2(t) + \mathbf{u}_2(t),\end{cases} \tag{30}$$

where $\mathbf{u}_2(t) := \mathbf{S}_3\left(\tilde{\mathbf{b}}_{\boldsymbol{\omega}}(t)\right)\boldsymbol{x}_2(t)$.

The following theorem is the main result of this section.

Theorem 3.3: *Consider the cascade attitude observer given by Equations* (18)*,* (19)*, and* (29)*. Then, in the conditions of Theorem* 3.1 *and Theorem* 3.2*, the origin of the observer error dynamics* (30) *is a GES equilibrium point.*

Proof: The proof follows exactly the same steps of Batista et al. (2012c, Theorem 3) and, therefore, it is omitted, even though the specific system dynamics are different. It is omitted due to space limitations.

3.4. Further discussion

3.4.1. Estimates on SO(3)

The attitude solution previously proposed does not yield estimates on $SO(3)$ as the special orthogonal group restrictions have been relaxed, in a similar fashion to the approaches proposed in Batista et al. (2012a) or Batista et al. (2012c). In the absence of noise, the estimates converge asymptotically to elements of $SO(3)$, while in the presence of noise their distance to $SO(3)$ remains close to zero. Additional refinements are possible such as those discussed in Batista et al. (2012c, Section 3.4). This is not the focus of the paper and as such it is omitted. Furthermore, explicit estimates on $SO(3)$ could be obtained, based in the attitude observer here proposed, resorting to Batista et al. (2012b, Theorem 7).

3.4.2. Computational complexity

The design herein proposed consists in a cascade observer where the number of states of the second observer is 9 and the number of states of the first observer is $N(N-1)M(M-1)/4 + 3$, with a total number of states of $N(N-1)M(M-1)/4 + 12$. For a typical LBL/USBL configuration with four landmarks and four acoustic receivers in the USBL array, that corresponds to 48 states. While this number may seem relatively high, it is very important to stress that the resulting observer is computationally efficient and of simple implementation. Indeed, all the observer coefficients are computed offline and no differential equations are required to compute the observer gains.

4. Position and linear velocity estimation

This section addresses the design of an estimation solution for the inertial position and inertial ocean current velocity based on the LBL/USBL positioning system assuming exact angular information, i.e., assuming that both the attitude and the angular velocity are available. First, state and output augmentation are performed, in Section 4.1, to attain a nominal system that, although nonlinear, can be regarded as linear for observability analysis and observer design purposes. Afterwards, the observability of that system is analysed in Section 4.2. Finally, in Section 4.3, a Kalman filter for the resulting system, with GES error dynamics, is briefly discussed.

4.1. State and output augmentation

In the recent past, a novel observer analysis and design technique has been proposed by the authors for navigation systems based on nonlinear range measurements, which consists basically of: (1) including the range measurements in the system state; (2) identifying the nonlinear terms of the dynamics of the range measurements as additional state variables; (3) defining augmented outputs, when appropriate, to capture the structure of arrays of landmarks or receivers; and (4) working with the resulting nonlinear system, which can actually be regarded as LTV, for observability analysis and observer design purposes. This approach has been successfully employed considering single measurements, see Batista et al. (2011b), LBL configurations, see Batista, Silvestre, and Oliveira (2010b, 2014), and USBL configurations, see Morgado et al. (2011), where different auxiliary sensors were considered, for example DVLs or triads of accelerometers. The design presented herein consists of the integration of both LBL/USBL measurements with this approach.

The time derivative of the range measurements (5) is given by

$$\dot{r}_{i,j}(t) = \frac{\mathbf{u}(t) + \mathbf{R}(t)\mathbf{S}(\boldsymbol{\omega}(t))\,\mathbf{a}_j}{r_{i,j}(t)} \cdot \mathbf{p}(t) + \frac{-\mathbf{s}_i + \mathbf{R}(t)\mathbf{a}_j}{r_{i,j}(t)} \cdot {}^{I}\mathbf{v}_c(t) + \frac{1}{r_{i,j}(t)}\mathbf{p}(t) \cdot {}^{I}\mathbf{v}_c(t) + u_{r_{i,j}}(t), \tag{31}$$

where

$$u_{r_{i,j}}(t) := \frac{\mathbf{u}^T(t)\mathbf{R}(t)\mathbf{a}_j - \mathbf{u}^T(t)\mathbf{s}_i - \mathbf{s}_i^T\mathbf{R}(t)\mathbf{S}(\boldsymbol{\omega}(t))\,\mathbf{a}_j}{r_{i,j}(t)}.$$

Identifying the nonlinear term $\mathbf{p}(t) \cdot {}^{I}\mathbf{v}_c(t)$ in Equation (31) with a new variable and taking its time derivative gives

$$\frac{d}{dt}\left[\mathbf{p}(t) \cdot {}^{I}\mathbf{v}_c(t)\right] = \mathbf{u}(t) \cdot {}^{I}\mathbf{v}_c(t) + \left\| {}^{I}\mathbf{v}_c(t)\right\|^2. \tag{32}$$

Finally, identifying the nonlinear term $\| {}^{I}\mathbf{v}_c(t)\|^2$ in Equation (32) and taking its time derivative gives $\frac{d}{dt}[\| {}^{I}\mathbf{v}_c(t)\|^2] = 0$.

For the sake of clarity of presentation, let $x_{1,1}(t) := r_{1,1}(t), \ldots, x_{N,M}(t) := r_{N,M}(t), x_3(t) := \mathbf{p}(t) \cdot {}^{I}\mathbf{v}_c(t)$, and $x_4(t) := \| {}^{I}\mathbf{v}_c(t)\|^2$, and define the augmented state vector as

$$\boldsymbol{x}_3(t) := \left[\mathbf{p}^T(t)\ {}^{I}\mathbf{v}_c^T(t) x_{1,1}(t) x_{1,2}(t) \ldots x_{N,M}(t)\ x_3(t) x_4(t)\right]^T \in \mathbb{R}^{3+3+NM+1+1}.$$

Then, the system dynamics can be written as

$$\dot{\boldsymbol{x}}_3(t) := \mathbf{A}_3(t)\boldsymbol{x}_3(t) + \mathbf{B}_3\mathbf{u}_a(t),$$

where $\mathbf{A}_3(t) \in \mathbb{R}^{(6+NM+2)\times(6+NM+2)}$,

$$\mathbf{A}_3(t) = \begin{bmatrix} \mathbf{0} & \mathbf{I} & \mathbf{0} & \mathbf{0} & \mathbf{0} \\ \mathbf{0} & \mathbf{0} & \mathbf{0} & \mathbf{0} & \mathbf{0} \\ \frac{\mathbf{u}^T(t) - \mathbf{a}_1^T\mathbf{S}(\boldsymbol{\omega}(t))\mathbf{R}^T(t)}{r_{1,1}(t)} & \frac{-\mathbf{s}_1^T + \mathbf{a}_1^T\mathbf{R}^T(t)}{r_{1,1}(t)} & \mathbf{0} & \frac{1}{r_{1,1}(t)} & 0 \\ \vdots & \vdots & \vdots & \vdots & \vdots \\ \frac{\mathbf{u}^T(t) - \mathbf{a}_M^T\mathbf{S}(\boldsymbol{\omega}(t))\mathbf{R}^T(t)}{r_{N,M}(t)} & \frac{-\mathbf{s}_N^T + \mathbf{a}_M^T\mathbf{R}^T(t)}{r_{N,M}(t)} & \mathbf{0} & \frac{1}{r_{N,M}(t)} & 0 \\ \mathbf{0} & \mathbf{u}^T(t) & \mathbf{0} & 0 & 1 \\ \mathbf{0} & \mathbf{0} & \mathbf{0} & 0 & 0 \end{bmatrix},$$

$$\mathbf{B}_3 = \begin{bmatrix} \mathbf{I}\ \mathbf{0} \\ \mathbf{0}\ \mathbf{0} \\ \mathbf{0}\ \mathbf{I} \\ \mathbf{0}\ \mathbf{0} \\ \mathbf{0}\ \mathbf{0} \end{bmatrix} \in \mathbb{R}^{(6+NM+2)\times(3+NM)},$$

and

$$\mathbf{u}_a(t) := \left[\mathbf{u}^T(t)\ u_{r_{1,1}}(t) \ldots u_{r_{N,M}}(t)\right]^T \in \mathbb{R}^{3+NM}.$$

To define the output, notice first that the states $x_{1,1}(t), \ldots, x_{N,M}(t)$ are measured. Note, however, that the RDOA between pairs of receivers to the same landmark are measured more accurately with the USBL when compared to the distance between the landmark and any given receiver of the USBL. Selecting a reference sensor on the array, for instance receiver 1 for now, all the other ranges are easily reconstructed from the range measured at receiver 1 and the RDOA between receiver 1 and the other receivers. Hence, the first set of measurements that is considered is

$$\mathbf{y}_1(t) = \begin{bmatrix} r_{1,1}(t) \\ r_{1,1}(t) - r_{1,2}(t) \\ \vdots \\ r_{1,1}(t) - r_{1,M}(t) \\ \vdots \\ r_{N,1}(t) \\ \vdots \\ r_{N,1}(t) - r_{N,M}(t) \end{bmatrix} \in \mathbb{R}^{NM}. \tag{33}$$

However, if that was the only output to be considered, the LBL/USBL structure would not be encoded in the output. To capture the LBL/USBL structure, consider first the square of the range measurements, which is given by

$$r_{i,j}^2(t) = \|\mathbf{p}(t)\|^2 + \|\mathbf{s}_i\|^2 + \|\mathbf{a}_j\|^2 - 2[\mathbf{s}_i - \mathbf{R}(t)\mathbf{a}_j] \cdot \mathbf{p}(t) - 2\mathbf{s}_i^T\mathbf{R}(t)\mathbf{a}_j$$

for all $i = 1, \ldots, N, j = 1, \ldots, M$. Then,

$$r_{m,j}^2(t) - r_{n,j}^2(t) = \|\mathbf{s}_m\|^2 - \|\mathbf{s}_n\|^2 - 2(\mathbf{s}_m - \mathbf{s}_n) \cdot [\mathbf{p}(t) + \mathbf{R}(t)\mathbf{a}_j] \tag{34}$$

and

$$r_{i,m}^2(t) - r_{i,n}^2(t) = \|\mathbf{a}_m\|^2 - \|\mathbf{a}_n\|^2 - 2[\mathbf{R}(t)(\mathbf{a}_m - \mathbf{a}_n)] \cdot [\mathbf{s}_i - \mathbf{p}(t)]. \tag{35}$$

Breaking the differences of the squares, using $a^2 - b^2 = (a + b)(a - b)$, it follows from Equations (34) and (35) that

$$2\frac{(\mathbf{s}_m - \mathbf{s}_n)^T}{r_{m,j}(t) + r_{n,j}(t)}\mathbf{p}(t) + x_{m,j}(t) - x_{n,j}(t) = \frac{\|\mathbf{s}_m\|^2 - \|\mathbf{s}_n\|^2 - 2(\mathbf{s}_m - \mathbf{s}_n)^T\mathbf{R}(t)\mathbf{a}_j}{r_{m,j}(t) + r_{n,j}(t)} \tag{36}$$

and

$$-2\frac{(\mathbf{a}_m - \mathbf{a}_n)^T\mathbf{R}^T(t)}{r_{i,m}(t) + r_{i,n}(t)}\mathbf{p}(t) + x_{i,m}(t) - x_{i,n}(t) = \frac{\|\mathbf{a}_m\|^2 - \|\mathbf{a}_n\|^2 - 2(\mathbf{a}_m - \mathbf{a}_n)^T\mathbf{R}^T(t)\mathbf{s}_i}{r_{i,m}(t) + r_{i,n}(t)}, \tag{37}$$

which capture the LBL/USBL structure. The augmented output can then be written as

$$\mathbf{y}_3(t) = \mathbf{C}_3(t)\boldsymbol{x}_3(t),$$

with $\mathbf{C}_3(t) \in \mathbb{R}^{\left(NM+M\,{}_2^N C+N\,{}_2^M C\right)\times(3+3+NM+1+1)}$,

$$\mathbf{C}_3(t) = \begin{bmatrix} \mathbf{0} & \mathbf{0} & \mathbf{C}_{13} & \mathbf{0} & \mathbf{0} \\ \mathbf{C}_{21}(t) & \mathbf{0} & \mathbf{C}_{23} & \mathbf{0} & \mathbf{0} \\ \mathbf{C}_{31}(t) & \mathbf{0} & \mathbf{C}_{33} & \mathbf{0} & \mathbf{0} \end{bmatrix},$$

where $\mathbf{C}_{13} := \operatorname{diag}\left(\mathbf{C}_{13}^0, \ldots, \mathbf{C}_{13}^0\right) \in \mathbb{R}^{\mathrm{NM}\times\mathrm{NM}}$, with

$$\mathbf{C}_{13}^0 := \begin{bmatrix} 1 & 0 & \ldots & \ldots & 0 \\ 1 & -1 & \ddots & & \vdots \\ 1 & 0 & -1 & \ddots & \vdots \\ \vdots & \vdots & \ddots & \ddots & 0 \\ 1 & 0 & \ldots & 0 & -1 \end{bmatrix} \in \mathbb{R}^{M\times M},$$

$$\mathbf{C}_{21}(t) := \begin{bmatrix} \mathbf{C}_{21}^1(t) \\ \vdots \\ \mathbf{C}_{21}^M(t) \end{bmatrix} \in \mathbb{R}^{\left(M\,{}_2^N C\right)\times 3},$$

$$\mathbf{C}_{21}^i(t) := 2\begin{bmatrix} \frac{(\mathbf{s}_1-\mathbf{s}_2)^T}{r_{1,i}(t)+r_{2,i}(t)} \\ \frac{(\mathbf{s}_1-\mathbf{s}_3)^T}{r_{1,i}(t)+r_{3,i}(t)} \\ \vdots \\ \frac{(\mathbf{s}_{N-1}-\mathbf{s}_N)^T}{r_{N-1,i}(t)+r_{N,i}(t)} \end{bmatrix} \in \mathbb{R}^{\,{}_2^N C\times 3},$$

$$\mathbf{C}_{31}(t) := \begin{bmatrix} \mathbf{C}_{31}^1(t) \\ \vdots \\ \mathbf{C}_{31}^N(t) \end{bmatrix} \in \mathbb{R}^{\left(N\,{}_2^M C\right)\times 3},$$

$$\mathbf{C}_{31}^i(t) := -2\begin{bmatrix} \frac{(\mathbf{a}_1-\mathbf{a}_2)^T\mathbf{R}^T(t)}{r_{i,1}(t)+r_{i,2}(t)} \\ \frac{(\mathbf{a}_1-\mathbf{a}_3)^T\mathbf{R}^T(t)}{r_{i,1}(t)+r_{i,3}(t)} \\ \vdots \\ \frac{(\mathbf{a}_{M-1}-\mathbf{a}_M)^T\mathbf{R}^T(t)}{r_{i,M-1}(t)+r_{i,M}(t)} \end{bmatrix} \in \mathbb{R}^{\,{}_2^M C\times 3},$$

where ${}_2^N C = N(N-1)/2$ and ${}_2^M C = M(M-1)/2$ correspond to the numbers of two-combinations of N and M elements, respectively, and $\mathbf{C}_{23}$ and $\mathbf{C}_{33}$ encode the differences of range measurements in Equations (36) and (37), respectively, which are omitted as they are evident from the context. In short, $\mathbf{C}_{31}$ encodes Equation (33), matrices $\mathbf{C}_{21}(t)$ and $\mathbf{C}_{23}$ encode Equation (36) for all $j \in \{1, \ldots, M\}$ and $m, n \in \{1, \ldots, N\}$, with $n \neq m$, and matrices $\mathbf{C}_{31}(t)$ and $\mathbf{C}_{33}$ encode Equation (37) for all $i \in \{1, \ldots, N\}$ and $m, n \in \{1, \ldots, M\}$, with $n \neq m$.

Considering the augmented system state and outputs, the final augmented system dynamics can be written as

$$\begin{cases} \dot{\boldsymbol{x}}_3(t) = \mathbf{A}_3(t)\boldsymbol{x}_3(t) + \mathbf{B}_3\mathbf{u}_a(t) \\ \mathbf{y}_3(t) = \mathbf{C}_3(t)\boldsymbol{x}_3(t) \end{cases}. \tag{38}$$

4.2. Observability analysis

The observability of the nonlinear system (38) and its relation with the original nonlinear system

$$\begin{cases} \dot{\mathbf{p}}(t) = {}^I\mathbf{v}_c(t) + \mathbf{u}(t) \\ {}^I\dot{\mathbf{v}}_c(t) = \mathbf{0}(t) \\ r_{1,1}(t) = \|\mathbf{s}_1 - \mathbf{p}(t) - \mathbf{R}(t)\mathbf{a}_1\| \\ \vdots \\ r_{N,M}(t) = \|\mathbf{s}_N - \mathbf{p}(t) - \mathbf{R}(t)\mathbf{a}_M\| \end{cases}. \tag{39}$$

is analysed in this section.

Even though the system dynamics (38) resemble an LTV system, it is, in fact, nonlinear, as the system matrices depend both on the output and the input. However, this is not a problem for observability and observer design purposes and the results for LTV systems still apply, see Batista et al. (2011b, Lemma 1). Before presenting the main results, it is, therefore, convenient to compute the transition matrix associated with $\mathbf{A}_3(t)$ and the observability Gramian associated with the pair $(\mathbf{A}_3(t), \mathbf{C}_3(t))$. Long, tedious but straightforward computations allow to show that the transition matrix associated with $\mathbf{A}_3(t)$ is given by

$$\boldsymbol{\phi}(t, t_0) = \begin{bmatrix} \boldsymbol{\phi}_A(t, t_0) & \mathbf{0} & \mathbf{0} \\ \boldsymbol{\phi}_{BA}(t, t_0) & \mathbf{I} & \boldsymbol{\phi}_{BC}(t, t_0) \\ \boldsymbol{\phi}_{CA}(t, t_0) & \mathbf{0} & \boldsymbol{\phi}_{CC}(t, t_0) \end{bmatrix},$$

where

$$\boldsymbol{\phi}_A(t, t_0) = \begin{bmatrix} \mathbf{I} & (t-t_0)\mathbf{I} \\ \mathbf{0} & \mathbf{I} \end{bmatrix} \in \mathbb{R}^{6\times 6},$$

$$\boldsymbol{\phi}_{BA}(t, t_0) = \begin{bmatrix} \boldsymbol{\phi}_{BA1}(t, t_0) & \boldsymbol{\phi}_{BA2}(t, t_0) \end{bmatrix} \in \mathbb{R}^{NM\times 6},$$

$$\boldsymbol{\phi}_{BA1}(t, t_0) = \begin{bmatrix} \boldsymbol{\phi}_{BA1(1,1)}(t, t_0) \\ \vdots \\ \boldsymbol{\phi}_{BA1(N,M)}(t, t_0) \end{bmatrix} \in \mathbb{R}^{NM\times 3},$$

$$\boldsymbol{\phi}_{BA1(i,j)}(t, t_0) = \int_{t_0}^{t} \frac{\mathbf{u}^T(\sigma) - \mathbf{a}_j^T\mathbf{S}(\boldsymbol{\omega}(\sigma))\mathbf{R}^T(\sigma)}{r_{i,j}(\sigma)} d\sigma,$$

$$\boldsymbol{\phi}_{BA2}(t,t_0)=\begin{bmatrix}\boldsymbol{\phi}_{BA2(1,1)}(t,t_0)\\ \vdots\\ \boldsymbol{\phi}_{BA2(N,M)}(t,t_0)\end{bmatrix}\in\mathbb{R}^{NM\times 3},$$

$$\boldsymbol{\phi}_{BA2(i,j)}(t,t_0)=\int_{t_0}^{t}\frac{-\mathbf{s}_i^T+\mathbf{a}_j^T\mathbf{R}^T(\sigma_1)}{r_{i,j}(\sigma)}d\sigma_1+\int_{t_0}^{t}\frac{(\sigma-t_0)\left[\mathbf{u}(\sigma_1)+\mathbf{R}(\sigma_1)\mathbf{S}(\boldsymbol{\omega}(\sigma_1))\mathbf{a}_j\right]^T+\int_{t_0}^{\sigma_1}\mathbf{u}^T(\sigma_2)d\sigma_2}{r_{i,j}(\sigma)}d\sigma_1,$$

$$\boldsymbol{\phi}_{BC}(t,t_0)=\begin{bmatrix}\int_{t_0}^{t}\frac{1}{r_{1,1}(\sigma)}d\sigma & \int_{t_0}^{t}\frac{\sigma-t_0}{r_{1,1}(\sigma)}d\sigma\\ \vdots & \vdots\\ \int_{t_0}^{t}\frac{1}{r_{N,M}(\sigma)}d\sigma & \int_{t_0}^{t}\frac{\sigma-t_0}{r_{N,M}(\sigma)}d\sigma\end{bmatrix}\in\mathbb{R}^{NM\times 2},$$

$$\boldsymbol{\phi}_{CA}(t,t_0)=\begin{bmatrix}\mathbf{0} & \int_{t_0}^{t}\mathbf{u}^T(\sigma)d\sigma\\ \mathbf{0} & \mathbf{0}\end{bmatrix}\in\mathbb{R}^{2\times 6},$$

and

$$\boldsymbol{\phi}_{CC}(t,t_0)=\begin{bmatrix}1 & t-t_0\\ 0 & 1\end{bmatrix}\in\mathbb{R}^{2\times 2},$$

It is, however, easy to verify that $\boldsymbol{\phi}(t_0,t_0)=\mathbf{I}$ and $\frac{d}{dt}\boldsymbol{\phi}(t,t_0)=\mathbf{A}_3(t)\boldsymbol{\phi}(t,t_0)$. The observability Gramian associated with the pair $(\mathbf{A}_3(t),\mathbf{C}_3)$ is simply given by

$$\boldsymbol{\mathcal{W}}_3(t_0,t_f)=\int_{t_0}^{t_f}\boldsymbol{\phi}^T(t,t_0)\mathbf{C}_3^T(t)\mathbf{C}_3(t)\boldsymbol{\phi}(t,t_0)\,dt. \quad (40)$$

The following theorem addresses the observability of Equation (38).

Theorem 4.1: *Under Assumption 2.1 or 2.2 (or both), the nonlinear system* (38) *is observable on* $\mathcal{I}:=[t_0,t_f]$, $t_0<t_f$, *in the sense that, given the system input* $\{\mathbf{u}_a(t),\,t\in\mathcal{I}\}$ *and the system output* $\{\mathbf{y}_3(t),\,t\in\mathcal{I}\}$, *the initial condition* $\boldsymbol{x}_3(t_0)$ *is uniquely determined.*

Proof: The proof follows by contradiction. Suppose that the nonlinear system (38) is not observable in $\mathcal{I}$. Then, the observability Gramian $\boldsymbol{\mathcal{W}}(t_0,t_f)$ is not invertible, see Batista et al. (2011b, Lemma 1), which means that there exists a unit vector

$$\mathbf{d}=\begin{bmatrix}\mathbf{d}_1^T & \mathbf{d}_2^T & \mathbf{d}_3^T & d_4^T d_5\end{bmatrix}^T\in\mathbb{R}^{3+3+NM+1+1},$$

with $\mathbf{d}_1\in\mathbb{R}^3$, $\mathbf{d}_2\in\mathbb{R}^3$, $\mathbf{d}_3\in\mathbb{R}^{NM}$, and $d_4,d_5\in\mathbb{R}$, such that

$$\mathbf{d}^T\boldsymbol{\mathcal{W}}(t_0,t)\,\mathbf{d}=0 \quad (41)$$

for all $t\in\mathcal{I}$. Substituting Equation (40) in Equation (41) yields

$$\int_{t_0}^{t}\|\mathbf{C}_3(\tau)\boldsymbol{\phi}(\tau,t_0)\,\mathbf{d}\|^2=0 \quad (42)$$

for all $t\in\mathcal{I}$. Taking the time derivative of Equation (42) gives $\|\mathbf{C}_3(t)\boldsymbol{\phi}(t,t_0)\,\mathbf{d}\|^2=0$ for all $t\in\mathcal{I}$, which in turn implies that

$$\mathbf{C}_3(t)\boldsymbol{\phi}(t,t_0)\,\mathbf{d}=\mathbf{0} \quad (43)$$

for all $t\in\mathcal{I}$. With $t=t_0$ in Equation (43) gives

$$\begin{cases}\mathbf{C}_{13}\mathbf{d}_3=\mathbf{0}\\ \mathbf{C}_{21}(t_0)\,\mathbf{d}_1+\mathbf{C}_{23}\mathbf{d}_3=\mathbf{0}.\\ \mathbf{C}_{31}(t_0)\,\mathbf{d}_1+\mathbf{C}_{33}\mathbf{d}_3=\mathbf{0}\end{cases} \quad (44)$$

Notice first that $\mathbf{C}_{13}$ has full rank, which means that $\mathbf{d}_3=\mathbf{0}$. On the other hand, under Assumption 2.1 matrix $\mathbf{C}_{21}(t_0)$ has full rank, while under Assumption 2.2 matrix $\mathbf{C}_{31}(t_0)$ has full rank. Hence, under the conditions of the theorem, it has been shown so far that the only solution of Equation (44) is $\mathbf{d}_1=\mathbf{0}$ and $\mathbf{d}_3=\mathbf{0}$. Taking in the time derivative of Equation (43) gives $\frac{d}{dt}\mathbf{C}_3(t)\boldsymbol{\phi}(t,t_0)\,\mathbf{d}=\mathbf{0}$ for all $t\in\mathcal{I}$. In particular, for $t=t_0$, and considering $\mathbf{d}_1=\mathbf{0}$ and $\mathbf{d}_3=\mathbf{0}$, it is possible to write that

$$[-\mathbf{s}_i+\mathbf{R}(t_0)\,\mathbf{a}_j]^T\mathbf{d}_2+d_4=0 \quad (45)$$

for all $i\in\{1,\ldots,N\}$ and $j\in\{1,\ldots,M\}$. Now, under Assumption 2.1 or 2.2 (or both), it is possible to show that the only solution of Equation (45) is $\mathbf{d}_2=\mathbf{0}$ and $d_4=0$. Finally, taking the second time derivative of Equation (43), for $t=t_0$, and considering $\mathbf{d}_1=\mathbf{d}_2=\mathbf{0}$, $\mathbf{d}_3=\mathbf{0}$, and $d_4=0$, it is possible to show that it must also be $d_5=0$. However, this contradicts the hypothesis of existence of a unit vector $\mathbf{d}$ such that Equation (41) holds. Hence, by contradiction, the observability Gramian $\boldsymbol{\mathcal{W}}(t_0,t_f)$ is invertible and hence the nonlinear system (38) is observable in the sense established in the theorem, see Batista et al. (2011b, Lemma 1). □

The fact that Equation (38) is observable does not immediately entail that the nonlinear system (39) is observable nor that an observer for Equation (38) is also an observer for Equation (39), as there is nothing in the system dynamics (38) imposing the nonlinear algebraic relations that were at its own origin. Moreover, the range measurements as a nonlinear function of the state were also discarded. However, all that turns out to be true, as shown in the following theorem.

Theorem 4.2: *Under Assumption 1 or 2 (or both), the nonlinear system* (39) *is observable on* $\mathcal{I}:=[t_0,t_f]$, $t_0<t_f$, *in the sense that, given the system input* $\boldsymbol{u}(t)$ *and the system output* $r_{1,1}(t),\ldots,r_{N,M}(t)$ *for* $t\in\mathcal{I}$, *the initial condition* $\boldsymbol{p}(t_0)$ *and* ${}^I\boldsymbol{v}_c(t_0)$ *is uniquely determined. Moreover, the initial conditions of the augmented nonlinear system* (38)

match those of Equation (39) *and hence an observer with globally asymptotically stable error dynamics for Equation* (38) *is also an observer for Equation* (39)*, whose error converges to zero for all initial conditions.*

Proof: Let

$$\boldsymbol{x}_3(t_0) := \begin{bmatrix} \mathbf{p}'(t_0) \\ {}^I\mathbf{v}_c'(t_0) \\ x_{1,1}(t_0) \\ x_{1,2}(t_0) \\ \vdots \\ x_{N,M}(t_0) \\ x_3(t_0) \\ x_4(t_0) \end{bmatrix} \in \mathbb{R}^{3+3+NM+1+1}$$

be the initial condition of Equation (38), which, from Theorem 4.1, is uniquely determined, and let $\mathbf{p}(t_0)$ and ${}^I\mathbf{v}_c(t_0)$ be the initial condition of Equation (39). First, notice that it must be $x_{1,1}(t_0) = r_{1,1}(t_0)$, ..., $x_{N,M}(t_0) = r_{N,M}(t_0)$ as these states are actually measured. Moreover, evaluating the outputs of the nonlinear system (38) that capture the LBL and USBL structure, given by Equations (36) and (37), at $t = t_0$, gives

$$2\frac{(\mathbf{s}_m - \mathbf{s}_n)^T}{r_{m,j}(t_0) + r_{n,j}(t_0)}\mathbf{p}'(t_0) + x_{m,j}(t_0) - x_{n,j}(t_0) = \frac{\|\mathbf{s}_m\|^2 - \|\mathbf{s}_n\|^2 - 2(\mathbf{s}_m - \mathbf{s}_n)^T \mathbf{R}(t_0)\mathbf{a}_j}{r_{m,j}(t_0) + r_{n,j}(t_0)}$$

and

$$-2\frac{(\mathbf{a}_m - \mathbf{a}_n)^T \mathbf{R}^T(t_0)}{r_{i,m}(t_0) + r_{i,n}(t_0)}\mathbf{p}'(t_0) + x_{i,m}(t_0) - x_{i,n}(t_0) = \frac{\|\mathbf{a}_m\|^2 - \|\mathbf{a}_n\|^2 - 2(\mathbf{a}_m - \mathbf{a}_n)^T \mathbf{R}^T(t_0)\mathbf{s}_i}{r_{i,m}(t_0) + r_{i,n}(t_0)}$$

or, equivalently,

$$2(\mathbf{s}_m - \mathbf{s}_n)^T \mathbf{p}'(t_0) + r_{m,j}^2(t_0) - r_{n,j}^2(t_0) = \|\mathbf{s}_m\|^2 - \|\mathbf{s}_n\|^2 - 2(\mathbf{s}_m - \mathbf{s}_n)^T \mathbf{R}(t_0)\mathbf{a}_j \quad (46)$$

and

$$-2(\mathbf{a}_m - \mathbf{a}_n)^T \mathbf{R}^T(t_0)\mathbf{p}'(t_0) + r_{i,m}^2(t_0) - r_{i,n}^2(t_0) = \|\mathbf{a}_m\|^2 - \|\mathbf{a}_n\|^2 - 2(\mathbf{a}_m - \mathbf{a}_n)^T \mathbf{R}^T(t_0)\mathbf{s}_i. \quad (47)$$

Substituting Equations (34) and (35) in Equations (46) and (47), respectively, gives

$$2(\mathbf{s}_m - \mathbf{s}_n)^T [\mathbf{p}'(t_0) - \mathbf{p}(t_0)] = 0 \quad (48)$$

for all $m, n \in \{1, \ldots, N\}$, $n \neq n$, and

$$2(\mathbf{a}_m - \mathbf{a}_n)^T \mathbf{R}^T(t_0)[\mathbf{p}'(t_0) - \mathbf{p}(t_0)] = 0 \quad (49)$$

for all $m, n \in \{1, \ldots, M\}$, $n \neq n$. Now, it is possible to show that, under Assumption 1 the only solution of Equation (48) is $\mathbf{p}'(t_0) = \mathbf{p}(t_0)$, while under Assumption 2 the only solution of Equation (49) is also $\mathbf{p}'(t_0) = \mathbf{p}(t_0)$. Thus, so far it has been shown that

$$\begin{cases} \mathbf{p}'(t_0) = \mathbf{p}(t_0) \\ x_{1,1}(t_0) = r_{1,1}(t_0) \\ \vdots \\ x_{N,M}(t_0) = r_{N,M}(t_0) \end{cases}. \quad (50)$$

As a function of the initial state of Equation (39), the square of the range readings can actually be written as

$$\begin{aligned} r_{i,j}^2(t) = {} & \left\| \int_{t_0}^{t} \mathbf{u}(\tau)\, d\tau \right\|^2 + 2[\mathbf{u}(t) + \mathbf{R}(t)\mathbf{a}_j] \cdot \mathbf{p}(t_0) \\ & + 2(t - t_0)\left[-\mathbf{s}_i + \mathbf{R}(t)\mathbf{a}_j + \int_{t_0}^{t} \mathbf{u}(\sigma)\, d\sigma \right] \\ & \cdot {}^I\mathbf{v}_c(t_0) + 2(t - t_0)\mathbf{p}(t_0) \cdot {}^I\mathbf{v}_c(t_0) \\ & + (t - t_0)^2 \| {}^I\mathbf{v}_c(t_0) \|^2 + r_{i,j}^2(t_0) \\ & - 2\mathbf{p}^T(t_0)\mathbf{R}(t_0)\mathbf{a}_j + 2\mathbf{s}_i^T \mathbf{R}(t_0)\mathbf{a}_j - 2\mathbf{s}_i^T \mathbf{R}(t)\mathbf{a}_j \\ & - 2[\mathbf{s}_i - \mathbf{R}(t)\mathbf{a}_j] \cdot \int_{t_0}^{t} \mathbf{u}(\tau)\, d\tau, \end{aligned} \quad (51)$$

while as a function of the initial states of Equation (38), it is possible to write

$$\begin{aligned} r_{i,j}^2(t) = {} & \left\| \int_{t_0}^{t} \mathbf{u}(\tau)\, d\tau \right\|^2 + 2[\mathbf{u}(t) + \mathbf{R}(t)\mathbf{a}_j] \cdot \mathbf{p}'(t_0) \\ & + 2(t - t_0)\left[-\mathbf{s}_i + \mathbf{R}(t)\mathbf{a}_j + \int_{t_0}^{t} \mathbf{u}(\sigma)\, d\sigma \right] \\ & \cdot {}^I\mathbf{v}_c'(t_0) + 2(t - t_0)x_3(t_0) + (t - t_0)^2 x_4(t_0) \\ & + x_{i,j}^2(t_0) - 2\mathbf{x}_1^T(t_0)\mathbf{R}(t_0)\mathbf{a}_j + 2\mathbf{s}_i^T \mathbf{R}(t_0)\mathbf{a}_j \\ & - 2\mathbf{s}_i^T \mathbf{R}(t)\mathbf{a}_j - 2[\mathbf{s}_i - \mathbf{R}(t)\mathbf{a}_j] \cdot \int_{t_0}^{t} \mathbf{u}(\tau)\, d\tau. \end{aligned} \quad (52)$$

Now, comparing the differences of the squares of the ranges $r_{m,j}^2(t) - r_{n,j}^2(t)$ and $r_{i,m}^2(t) - r_{i,n}^2(t)$, using Equations (50)–(52), it is possible to write

$$\begin{cases} [\mathbf{s}_i - \mathbf{s}_j]^T \left[{}^I\mathbf{v}_c'(t_0) - {}^I\mathbf{v}_c(t_0) \right] = 0 \\ [\mathbf{a}_m - \mathbf{a}_n]^T \mathbf{R}^T(t) \left[{}^I\mathbf{v}_c'(t_0) - {}^I\mathbf{v}_c(t_0) \right] = 0 \end{cases} \quad (53)$$

for all $i, j \in \{1, \ldots, N\}$, $i \neq j$, and all $m, n \in \{1, \ldots, M\}$, $m \neq n$. Under Assumption 2.1 or 2.2, or both, the only solution

of Equation (53) is

$$ {}^{I}\mathbf{v}_c'(t_0) = {}^{I}\mathbf{v}_c(t_0). \tag{54} $$

Now, comparing Equations (51) with Equation (52) and using (50) and (54) it follows that

$$ \begin{aligned} &2(t-t_0)\left[x_3(t_0) - \mathbf{p}(t_0)\cdot {}^{I}\mathbf{v}_c(t_0)\right] \\ &+ (t-t_0)^2\left[x_4(t_0) - \| {}^{I}\mathbf{v}_c(t_0)\|^2\right] = 0. \end{aligned} \tag{55} $$

As the functions $2(t-t_0)$ and $(t-t_0)^2$ are linearly independent, it follows from Equation (55) that

$$ \begin{cases} x_3(t_0) = \mathbf{p}(t_0)\cdot {}^{I}\mathbf{v}_c(t_0) \\ x_4(t_0) = \| {}^{I}\mathbf{v}_c(t_0)\|^2 \end{cases}. $$

However, this concludes the proof: (1) it has been shown that the initial conditions of Equation (39) match those of Equation (38), which are uniquely determined as shown in Theorem 4.1, hence concluding the proof of the first part of the theorem; and (2) the second part of the theorem follows from the first: the estimation error of an observer for Equation (38) with globally asymptotically stable error dynamics converges to zero, which means that its estimates asymptotically approach the true state. However, as the true state of Equation (38) matches that of the nonlinear system (39), that means that an observer for Equation (38) is also an observer for the original nonlinear system, whose error converges to zero for all initial conditions.

4.3. Kalman filter

As a result of Theorem 4.2, a filtering solution for the nonlinear system (39) is simply obtained with the design of a Kalman filter for the augmented system (38), which can be regarded as LTV for this purpose as the output and input are available. The design is trivial and therefore it is omitted. Notice that the proposed solution is not an EKF, which would not offer global convergence guarantees, and no approximate linearisations are carried out.

To guarantee that the Kalman filter has GES error dynamics, stronger forms of observability are required, in particular uniform complete observability, see Sastry and Desoer (1982) and Jazwinski (1970). The pair $(\mathbf{A}_3(t), \mathbf{C}_3(t))$ can be shown to be uniformly completely observable following the same reasoning as in Theorem 4.1 but considering uniform bounds. The proof is omitted due to the lack of space.

5. Integrated LBL/USBL navigation system

In Section 3, a cascade observer was proposed for the attitude based on the measurements provided by the rate gyros and the LBL/USBL system, which gives in addition estimates of the rate gyro bias. The error dynamics were shown to be GES and the estimation system does not depend on any other quantities. In Section 4, the problem of estimating the linear motion quantities (inertial position and ocean current velocity) was addressed assuming perfect angular information, i.e., assuming that the attitude and the angular velocity are known. In practice, these quantities are provided by the estimator developed in Section 3 and as such the overall LBL/USBL navigation system consists in a cascade system, where the attitude observer feeds the position and velocity filter, as depicted in Figure 2. In short, the rate gyro bias estimate is employed to obtain an estimate of the angular velocity, which is fed, together with the estimate of the attitude, to the estimator for linear motion quantities.

The fact that the exact values of $\mathbf{R}(t)$ and $\boldsymbol{\omega}(t)$ are not available for the Kalman filter proposed in Section 4.3 induces errors in the system matrices $\mathbf{A}_3(t)$ and $\mathbf{C}_3(t)$, as well as in the system input $\mathbf{u}_a(t)$, and only estimates of these quantities are available, i.e., the Kalman filter for the estimation of linear motion quantities has available

$$ \hat{\mathbf{A}}_3(t) = \begin{bmatrix} \mathbf{0} & \mathbf{I} & \mathbf{0} & \mathbf{0} & \mathbf{0} \\ \mathbf{0} & \mathbf{0} & \mathbf{0} & \mathbf{0} & \mathbf{0} \\ \frac{\hat{\mathbf{u}}^T(t) - \mathbf{a}_1^T \mathbf{S}(\hat{\boldsymbol{\omega}}(t))\hat{\mathbf{R}}^T(t)}{r_{1,1}(t)} & \frac{-\mathbf{s}_1^T + \mathbf{a}_1^T \hat{\mathbf{R}}^T(t)}{r_{1,1}(t)} & \mathbf{0} & \frac{1}{r_{1,1}(t)} & 0 \\ \vdots & \vdots & \vdots & \vdots & \vdots \\ \frac{\hat{\mathbf{u}}^T(t) - \mathbf{a}_M^T \mathbf{S}(\hat{\boldsymbol{\omega}}(t))\hat{\mathbf{R}}^T(t)}{r_{N,M}(t)} & \frac{-\mathbf{s}_N^T + \mathbf{a}_M^T \hat{\mathbf{R}}^T(t)}{r_{N,M}(t)} & \mathbf{0} & \frac{1}{r_{N,M}(t)} & 0 \\ \mathbf{0} & \hat{\mathbf{u}}^T(t) & \mathbf{0} & 0 & 1 \\ \mathbf{0} & \mathbf{0} & \mathbf{0} & 0 & 0 \end{bmatrix}, $$

instead of $\mathbf{A}_3(t)$,

$$ \hat{\mathbf{C}}_3(t) = \begin{bmatrix} \mathbf{0} & \mathbf{0} & \mathbf{C}_{13} & \mathbf{0} & \mathbf{0} \\ \mathbf{C}_{21}(t) & \mathbf{0} & \mathbf{C}_{23} & \mathbf{0} & \mathbf{0} \\ \hat{\mathbf{C}}_{31}(t) & \mathbf{0} & \mathbf{C}_{33} & \mathbf{0} & \mathbf{0} \end{bmatrix} $$

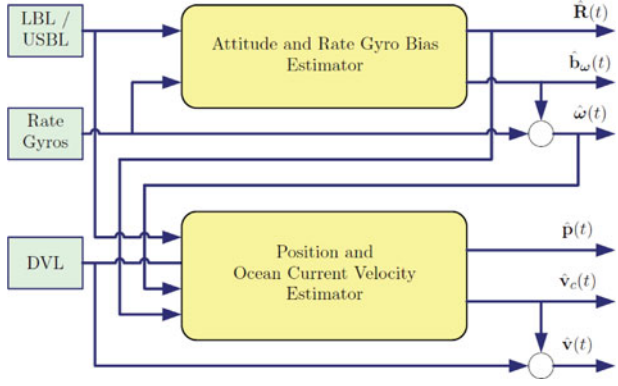

Figure 2. Integrated LBL/USBL navigation system.

instead of $\mathbf{C}_3(t)$, with

$$\hat{\mathbf{C}}_{31}(t) := \begin{bmatrix} \hat{\mathbf{C}}_{31}^1(t) \\ \vdots \\ \hat{\mathbf{C}}_{31}^N(t) \end{bmatrix} \in \mathbb{R}^{\left(N\,\frac{M}{2}C\right)\times 3},$$

$$\hat{\mathbf{C}}_{31}^i(t) := -2\begin{bmatrix} \frac{(\mathbf{a}_1-\mathbf{a}_2)^T\hat{\mathbf{R}}^T(t)}{r_{i,1}(t)+r_{i,2}(t)} \\ \frac{(\mathbf{a}_1-\mathbf{a}_3)^T\hat{\mathbf{R}}^T(t)}{r_{i,1}(t)+r_{i,3}(t)} \\ \vdots \\ \frac{(\mathbf{a}_{M-1}-\mathbf{a}_M)^T\hat{\mathbf{R}}^T(t)}{r_{i,M-1}(t)+r_{i,M}(t)} \end{bmatrix} \in \mathbb{R}^{\frac{M}{2}C\times 3},$$

and

$$\hat{\mathbf{u}}_a(t) := \begin{bmatrix} \hat{\mathbf{u}}(t) \\ \hat{u}_{r_{1,1}}(t) \\ \vdots \\ \hat{u}_{r_{N,M}}(t) \end{bmatrix}$$

instead of $\mathbf{u}_a(t)$, with $\hat{\mathbf{u}}(t) := \hat{\mathbf{R}}(t)\mathbf{v}_r(t)$ and

$$\hat{u}_{r_{i,j}}(t) := \frac{\hat{\mathbf{u}}^T(t)\hat{\mathbf{R}}(t)\mathbf{a}_j - \hat{\mathbf{u}}^T(t)\mathbf{s}_i - \mathbf{s}_i^T\hat{\mathbf{R}}(t)\mathbf{S}\left(\hat{\boldsymbol{\omega}}(t)\right)\mathbf{a}_j}{r_{i,j}(t)}.$$

Moreover, the augmented measurements are also estimated, and

$$\hat{\mathbf{y}}_3(t) = \begin{bmatrix} \mathbf{y}_1(t) \\ \frac{\|\mathbf{s}_1\|^2-\|\mathbf{s}_2\|^2-2(\mathbf{s}_1-\mathbf{s}_2)^T\hat{\mathbf{R}}(t)\mathbf{a}_1}{r_{1,1}(t)+r_{2,1}(t)} \\ \frac{\|\mathbf{s}_1\|^2-\|\mathbf{s}_3\|^2-2(\mathbf{s}_1-\mathbf{s}_3)^T\hat{\mathbf{R}}(t)\mathbf{a}_1}{r_{1,1}(t)+r_{3,1}(t)} \\ \vdots \\ \frac{\|\mathbf{s}_{N-2}\|^2-\|\mathbf{s}_N\|^2-2(\mathbf{s}_{N-2}-\mathbf{s}_N)^T\hat{\mathbf{R}}(t)\mathbf{a}_M}{r_{N-2,M}(t)+r_{N,M}(t)} \\ \frac{\|\mathbf{s}_{N-1}\|^2-\|\mathbf{s}_N\|^2-2(\mathbf{s}_{N-1}-\mathbf{s}_N)^T\hat{\mathbf{R}}(t)\mathbf{a}_M}{r_{N-1,M}(t)+r_{N,M}(t)} \\ \frac{\|\mathbf{a}_1\|^2-\|\mathbf{a}_2\|^2-2(\mathbf{a}_1-\mathbf{a}_2)^T\hat{\mathbf{R}}^T(t)\mathbf{s}_1}{r_{1,1}(t)+r_{1,2}(t)} \\ \frac{\|\mathbf{a}_1\|^2-\|\mathbf{a}_3\|^2-2(\mathbf{a}_1-\mathbf{a}_3)^T\hat{\mathbf{R}}^T(t)\mathbf{s}_1}{r_{1,1}(t)+r_{1,3}(t)} \\ \vdots \\ \frac{\|\mathbf{a}_{M-2}\|^2-\|\mathbf{a}_M\|^2-2(\mathbf{a}_{M-2}-\mathbf{a}_M)^T\hat{\mathbf{R}}^T(t)\mathbf{s}_N}{r_{N,M-2}(t)+r_{N,M}(t)} \\ \frac{\|\mathbf{a}_{M-1}\|^2-\|\mathbf{a}_M\|^2-2(\mathbf{a}_{M-1}-\mathbf{a}_M)^T\hat{\mathbf{R}}^T(t)\mathbf{s}_N}{r_{N,M-1}(t)+r_{N,M}(t)} \end{bmatrix}$$

is employed instead of $\mathbf{y}_3(t)$.

Let $\mathbf{w}(t)$ denote the system disturbances, assumed as zero-mean white Gaussian noise, with $\mathrm{E}[\mathbf{w}(\mathrm{t})\,\mathbf{w}^{\mathrm{T}}(\mathrm{t}-\tau)] = \boldsymbol{\Xi}\delta(\tau)$, and $\mathbf{n}(t)$ be the output noise, assumed as zero-mean white Gaussian noise, with $\mathrm{E}[\mathbf{n}(\mathrm{t})\,\mathbf{n}^{\mathrm{T}}(\mathrm{t}-\tau)] = \boldsymbol{\Theta}\delta(\tau)$ and $\mathrm{E}[\mathbf{w}(\mathrm{t})\,\mathbf{n}^{\mathrm{T}}(\mathrm{t}-\tau)] = \mathbf{0}$. The resulting Kalman filter is given by

$$\dot{\hat{\boldsymbol{x}}}_3(t) = \hat{\mathbf{A}}_3(t)\hat{\boldsymbol{x}}_3(t) + \mathbf{B}_3\hat{\mathbf{u}}_a(t) + \hat{\mathbf{K}}(t)[\hat{\mathbf{y}}_3(t) - \hat{\mathbf{C}}_3(t)\hat{\boldsymbol{x}}_3(t)],$$

where $\hat{\mathbf{K}}(t)$ is the Kalman gain,

$$\hat{\mathbf{K}}(t) = \hat{\mathbf{P}}(t)\,\hat{\mathbf{C}}_3^T(t)\boldsymbol{\Theta}^{-1},$$

where $\hat{\mathbf{P}}(t)$ is the covariance matrix, which satisfies

$$\begin{aligned}\dot{\hat{\mathbf{P}}}(t) = {} & \hat{\mathbf{A}}_3(t)\,\hat{\mathbf{P}}(t) + \hat{\mathbf{P}}(t)\,\hat{\mathbf{A}}_3^T(t) + \boldsymbol{\Xi} \\ & - \hat{\mathbf{P}}(t)\,\hat{\mathbf{C}}_3^T(t)\boldsymbol{\Theta}^{-1}\hat{\mathbf{C}}_3(t)\hat{\mathbf{P}}(t).\end{aligned}$$

Naturally, it is necessary to show that the error of the perturbed Kalman filter converges to zero for all initial conditions. This is a theoretical problem, that of the study of the convergence of the error of the Kalman filter when the system matrices $\mathbf{A}(t)$ and $\mathbf{C}(t)$, as well as the system output $\mathbf{y}(t)$, are perturbed by exponential decaying errors. Assuming (1) bounds on the system matrices; (2) that the nominal system is uniformly completely observable; and (3) that the system state is bounded, it can actually be shown that the error of the Kalman filter converges exponentially fast for all initial conditions. This falls out of the scope of this paper and will be detailed in a future article. However, all required assumptions are verified, in practice, for the proposed LBL/USBL setup, as the mission scenario is bounded in space and the linear and angular velocities must also be bounded due to the actuation bounds of any real system.

6. Simulations

This section provides simulation results to demonstrate the achievable performance with the proposed solution. In the simulations, the three-dimensional kinematic model for an underwater vehicle was employed. It is not necessary to consider the dynamics as the estimators are purely kinematic, hence the results apply to all underwater vehicles, regardless of the dynamics. The trajectory described by the vehicle is shown in Figure 3. The LBL configuration is composed of four acoustic transponders and their inertial positions are $\mathbf{s}_1 = [\,0\;0\;0\,](\mathrm{m}), \mathbf{s}_2 = [\,0\;0\;250\,](\mathrm{m}), \mathbf{s}_3 = [1000\;0\;250\,](\mathrm{m}), \mathbf{s}_4 = [\,0\;1000\;250\,](\mathrm{m})$, while the positions of the USBL array receivers, in body-fixed coordinates, are $\mathbf{a}_1 = [\,0\;0\;0\,](\mathrm{m}), \mathbf{a}_2 = [\,0\;0.3\;0\,](\mathrm{m}), \mathbf{a}_3 = [0.20\;0.15\;0.15\,](\mathrm{m}), \mathbf{a}_4 = [\,0.20\;0.15\;-0.15\,](\mathrm{m})$, hence both Assumptions 2.1 and 2.2 are satisfied.

Sensor noise was considered for all sensors. In particular, the LBL range measurements, the USBL RDOA, and the DVL relative velocity readings are assumed to be corrupted by additive uncorrelated zero-mean white Gaussian noise, with standard deviations of 1 m, 6×10^{-3} m, and 0.01 m/s, respectively. The angular velocity measurements

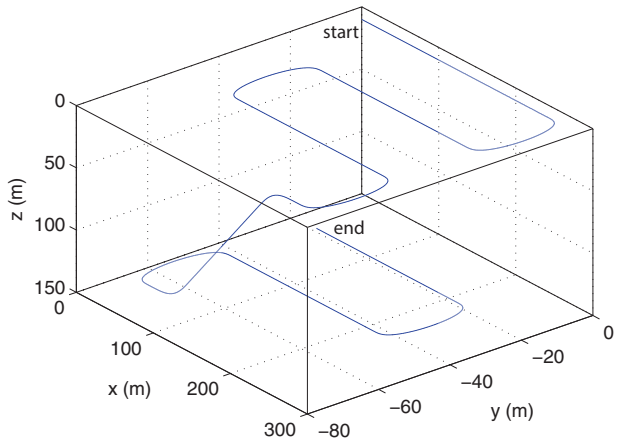

Figure 3. Trajectory described by the vehicle.

are also assumed to be perturbed by additive, zero mean, white Gaussian noise, with standard deviation of 0.05 °/s.

To tune the Kalman filter for the estimation of the linear motion quantities, the state disturbance intensity matrix was chosen as

$$\text{diag}(10^{-2}\mathbf{I},\ 10^{-4}\mathbf{I},\ 10^{-2},\ \ldots,\ 10^{-2},\ 10^{-2},\ 10^{-3})$$

and the output noise intensity matrix as

$$\text{diag}\left(\mathbf{Q}_0, \mathbf{Q}_0, \mathbf{Q}_0, \mathbf{Q}_0, 1, \ldots, 1\right),$$

where $\mathbf{Q}_0 := \text{diag}\,(1,\ 0.6,\ 0.6,\ 0.6)$. The parameters of the attitude observer were chosen as $\alpha(m, n, i, j) = 0.1$, $\beta(m, n, i, j) = 5\times10^{-8}$ for all $(m, n, i, j) \in \mathcal{C}_\mathbf{s} \times \mathcal{C}_\mathbf{a}$, and $\mathbf{Q} = 10^4\mathbf{I}$. All initial conditions were set to zero but the initial attitude estimate, which was set with a large error, with a rotation of 180 degrees about the z-axis.

The convergence of the attitude observer error is very fast, as it is possible to observe from the evolution of the errors of the components of the rotation matrix and the rate gyro bias error, which are depicted in Figure 4. The error of the additional states of the attitude observer, $\tilde{\mathbf{q}}(t)$ also converges and is not shown here only because it corresponds to intermediate states with no use in practice.

The initial evolution of the position and velocity errors are depicted in Figure 5. As it can be seen from the various plots, the convergence rate of the filter for the estimation of the linear motion quantities is quite fast.

To evaluate the performance of the attitude observer, and for the purpose of performance evaluation only, an additional error variable is defined as $\tilde{\mathbf{R}}_p(t) = \mathbf{R}^T(t)\hat{\mathbf{R}}(t)$, which corresponds to the rotation matrix error. Using the Euler angle-axis representation for this new error variable,

$$\tilde{\mathbf{R}}_p(t) = \mathbf{I}\cos\left(\tilde{\theta}(t)\right) + [1 - \cos\left(\tilde{\theta}(t)\right)]\tilde{\mathbf{d}}(t)\tilde{\mathbf{d}}^T(t) - \mathbf{S}\left(\tilde{\mathbf{d}}(t)\right)\sin\left(\tilde{\theta}(t)\right),$$

where $0 \leq \tilde{\theta}(t) \leq \pi$ and $\tilde{\mathbf{d}}(t) \in \mathbb{R}^3$, $\|\tilde{\mathbf{d}}(t)\| = 1$, are the angle and axis that represent the rotation error, the performance of the observer is identified with the evolution of $\tilde{\theta}$. After the initial transients fade out, the resulting angle mean error is around 0.06°.

Finally, to better evaluate the performance of the proposed solution, the Monte Carlo method was applied, and 1000 simulations were carried out with different, randomly generated noise signals. The standard deviation of the errors were computed for each simulation and averaged over the set of simulations. The results are depicted in Table 1. The mean attitude angle error is 0.05°. As it is possible to observe, the standard deviation of the errors is very low, adequate for the sensor suite that was considered.

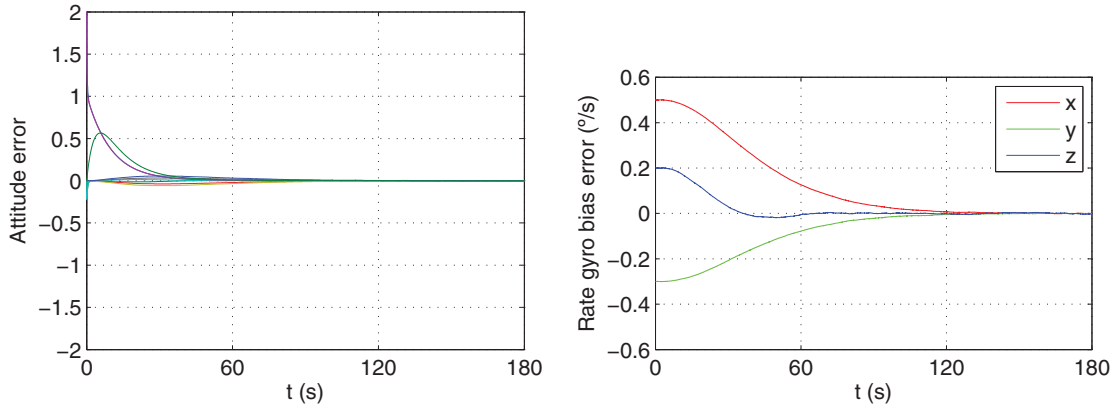

Figure 4. Initial convergence of the attitude observer errors $\tilde{\mathbf{R}}(t)$ and $\tilde{\mathbf{b}}_\omega(t)$.

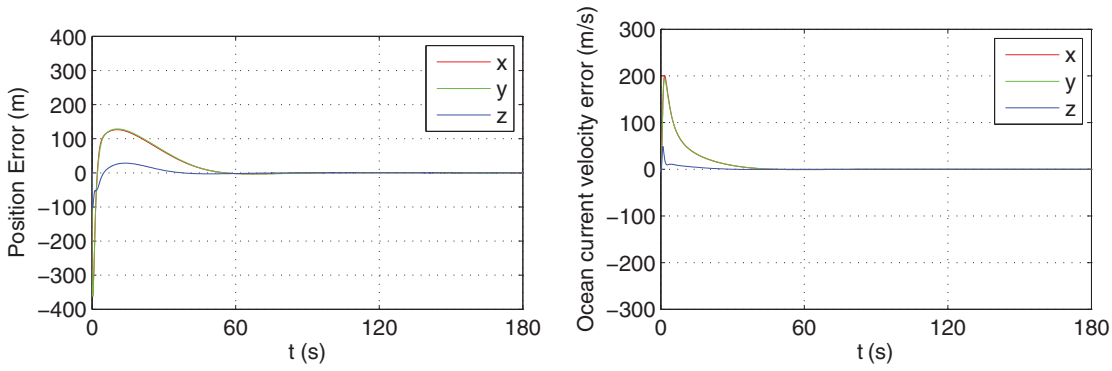

Figure 5. Initial convergence of the position error $\tilde{\mathbf{p}}(t)$ and the current velocity error $\tilde{\mathbf{v}}_c(t)$.

Table 1. Standard deviation of the steady-state estimation error, averaged over 1000 runs of the simulation.

Variable	Standard deviation
$\tilde{\mathbf{p}}_x$(m)	3.6×10^{-2}
$\tilde{\mathbf{p}}_y$(m)	4.0×10^{-2}
$\tilde{\mathbf{p}}_z$(m)	4.4×10^{-2}
$\tilde{\mathbf{v}}_x$(m/s)	2.3×10^{-3}
$\tilde{\mathbf{v}}_y$(m/s)	2.4×10^{-3}
$\tilde{\mathbf{v}}_z$(m/s)	3.0×10^{-3}
$\tilde{\mathbf{b}}_{\omega x}$ (°/s)	1.2×10^{-3}
$\tilde{\mathbf{b}}_{\omega y}$ (°/s)	0.9×10^{-3}
$\tilde{\mathbf{b}}_{\omega z}$ (°/s)	2.0×10^{-3}

7. Conclusions

This paper proposed a novel integrated tightly coupled navigation filter for autonomous vehicles based on a combined LBL/USBL positioning system. First, a rate gyro bias observer is proposed, which feeds a second attitude observer that yields estimates of the rotation matrix from body-fixed to inertial coordinates. The error of the cascade rate gyro bias and attitude observer was shown to be GES. Second, a framework for the estimation of the position of the vehicle and the ocean current velocity was proposed, which also features GES error dynamics assuming perfect knowledge of the attitude of the vehicle. This quantity is actually provided by the previous observer, which results in an overall cascade system. The structure is tightly coupled in the sense that the actual measurements of the LBL/USBL are directly employed in the estimator dynamics. Simulation results were carried out, including Monte Carlo simulations, that evidence excellent performance of the proposed solution in the presence of realistic sensor noise. Future work includes: (1) explicitly account for measurement delays; (2) comparison with the EKF, which does not offer global convergence guarantees; (3) design of an outlier rejection algorithm that takes advantage of the fact that each range or range difference of arrival is used directly in the filter, meaning that it is possible to exclude some measurements while still operating with the others; (4) study of the convergence of the error of the Kalman filter when the system matrices, as well as the system output, are perturbed by exponential decaying errors; and (5) experimental validation of the proposed estimation solution.

Funding

This work was supported by the FCT [grant number PEst-OE/EEI/LA0009/2013].

Notes on contributors

Pedro Batista received the Licenciatura degree in electrical and computer engineering in 2005 and the PhD degree in 2010, both from Instituto Superior Técnico (IST), Lisbon, Portugal. From 2004 to 2006, he was a monitor with the Department of Mathematics, IST, where he is currently an invited assistant professor with the Department of Electrical and Computer Engineering. His research interests include sensor-based navigation and control of autonomous vehicles. He has received the Diploma de Mérito twice during his graduation and his PhD thesis was awarded the Best Robotics PhD Thesis Award by the Portuguese Society of Robotics.

Carlos Silvestre received the Licenciatura degree in electrical engineering from the Instituto Superior Tecnico (IST) of Lisbon, Portugal, in 1987 and the MSc degree in Electrical Engineering and the PhD degree in Control Science from the same school in 1991 and 2000, respectively. In 2011, he received the habilitation in Electrical Engineering and Computers also from IST. Since 2000, he is with the Department of Electrical Engineering of the Instituto Superior Tecnico, where he is currently an associate professor of Control and Robotics on leave. Since 2012, he is an associate professor of the Department of Electrical and Computers Engineering of the faculty of Science and Technology of the University of Macau. Over the past years, he has conducted research on the subjects of navigation guidance and control of air and underwater robots. His research interests include linear and

nonlinear control theory, coordinated control of multiple vehicles, gain scheduled control, integrated design of guidance and control systems, inertial navigation systems, and mission control and real time architectures for complex autonomous systems with applications to unmanned air and underwater vehicles.

Paulo Oliveira completed the PhD in 2002 from the Instituto Superior Técnico, Lisbon, Portugal. He is associate professor of the Department of Mechanical Engineering, Instituto Superior Técnico, ULisboa, Lisbon, Portugal and senior researcher in the Institute for Systems and Robotics of LARSyS. The areas of scientific activity are Robotics and Autonomous Vehicles with special focus on the fields of Sensor Fusion, Navigation, Positioning, and Signal Processing. He participated in more than 15 Portuguese and European Research projects, over the last 20 years and published 200 journal and conference papers in his areas of research.

References

Alcocer, A., Oliveira, P., & Pascoal, A. (2007). Study and implementation of an EKF GIB-based underwater positioning system. *Control Engineering Practice, 15*(6), 689–701.

Batista, P., Silvestre, C., & Oliveira, P. (2009, June). Position and velocity optimal sensor-based navigation filters for UAVs. In *Proceedings of the 2009 American Control Conference* (pp. 5404–5409). Saint Louis.

Batista, P., Silvestre, C., & Oliveira, P. (2010a). Optimal position and velocity navigation filters for autonomous vehicles. *Automatica, 46*(4), 767–774.

Batista, P., Silvestre, C., & Oliveira, P. (2010b, September). A sensor-based long baseline position and velocity navigation filter for underwater vehicles. In *Proceedings of the 8th IFAC Symposium on Nonlinear Control Systems - NOLCOS 2010* (pp. 302–307). Bologna.

Batista, P., Silvestre, C., & Oliveira, P. (2011a, December). GES Integrated LBL/USBL navigation system for underwater vehicles. In *Proceedings of the 51st IEEE Conference on Decision and Control* (pp. 6609–6614). Hawaii.

Batista, P., Silvestre, C., & Oliveira, P. (2011b). Single range aided navigation and source localization: Observability and filter design. *Systems & Control Letters, 60*(8), 665–673.

Batista, P., Silvestre, C., & Oliveira, P. (2012a), "Sensor-based globally asymptotically stable filters for attitude estimation: Analysis, design, and performance evaluation. *IEEE Transactions on Automatic Control, 57*(8), 2095–2100.

Batista, P., Silvestre, C., & Oliveira, P. (2012b). A GES attitude observer with single vector observations. *Automatica, 48*(2), 388–395.

Batista, P., Silvestre, C., & Oliveira, P. (2012c). Globally exponentially stable cascade observers for attitude estimation. *Control Engineering Practice, 20*(2), 148–155.

Batista, P., Silvestre, C., & Oliveira, P. (2013a, July). GAS tightly coupled LBL/USBL position and velocity filter for underwater vehicles. In *Proceedings of the 2013 European Control Conference* (pp. 2982–2987). Zurich.

Batista, P., Silvestre, C., & Oliveira, P. (2013b, July). GES tightly coupled attitude estimation based on a LBL/USBL positioning system. In *Proceedings of the 2013 European Control Conference* (pp. 2988–2993). Zurich.

Batista, P., Silvestre, C., & Oliveira, P. (2014). Sensor-based long baseline navigation: Observability analysis and filter design. *Asian Journal of Control, 16*(3), 1–21.

Bhat, S., & Bernstein, D. (2000). A topological obstruction to continuous global stabilization of rotational motion and the unwinding phenomenon. *Systems & Control Letters, 39*(1), 63–70.

Campolo, D., Keller, F., & Guglielmelli, E. (2006, October). Inertial/Magnetic sensors based orientation tracking on the group of rigid body rotations with application to wearable devices. In *Proceedings of the 2006 IEEE/RSJ International Conference on Intelligent Robots and Systems - IROS 2006* (pp. 4762–4767). Beijing.

Choukroun, D. (2009, August). Novel results on quaternion modeling and estimation from vector observations. In *Proceedings of the AIAA Guidance Navigation and Control Conference*. Chicago, IL.

Grip, H., Fossen, T., Johansen, T., & Saberi, A. (2012). Attitude estimation using biased Gyro and vector measurements with time-varying reference vectors. *IEEE Transactions on Automatic Control, 57* (5), 1332–1338.

Ioannou, P., & Sun, J. (1995). *Robust adaptive control*. Upper Saddle River, NJ: Prentice Hall.

Jazwinski, A. (1970). *Stochastic processes and filtering theory*. New York, NY: Academic Press.

Jouffroy, J., & Opderbecke, J. (2004, June–July). Underwater vehicle trajectory estimation using contracting PDE-based observers. In *Proceedings of the 2004 American Control Conference* (Vol. 5, pp. 4108–4113). Boston, MA.

Khalil, H. (2001). *Nonlinear systems* (3rd ed.). Upper Saddle River, NJ: Prentice Hall.

Kinsey, J., Eustice, R., & Whitcomb, L. (2006, September). A survey of underwater vehicle navigation: Recent advances and new challenges. In *Proceedings of the 7th IFAC Conference on Manoeuvring and Control of Marine Craft*. Lisboa.

Kinsey, J., & Whitcomb, L. (2003, April). Preliminary field experience with the DVLNAV integrated navigation system for manned and unmanned submersibles. In *Proceedings of the 1st IFAC Workshop on Guidance and Control of Underwater Vehicles* (pp. 83–88). Newport, South Wales.

Larsen, M. (2000). Synthetic long baseline navigation of underwater vehicles. In *Proceedings of the 2000 MTS/IEEE Oceans* (Vol. 3, pp. 2043–2050). Providence, RI.

Leonard, J., Bennett, A., Smith, C., & Feder, H. (1998). *Autonomous underwater vehicle navigation* (Technical Report Technical Memorandum 98-1). Cambridge, MA: MIT Marine Robotics Laboratory.

Mahony, R., Hamel, T., & Pflimlin, J.M. (2008). Nonlinear complementary filters on the special orthogonal group. *IEEE Transactions on Automatic Control, 53*(5), 1203–1218.

Martin, P., & Salaun, E. (2010). Design and implementation of a low-cost observer-based attitude and heading reference system. *Control Engineering Practice, 17*(7), 712–722.

Metni, N., Pflimlin, J.M., Hamel, T., & Soueres, P. (2006). Attitude and gyro bias estimation for a VTOL UAV. *Control Engineering Practice, 14*(12), 1511–1520.

Morgado, M., Batista, P., Oliveira, P., & Silvestre, C. (2011). Position USBL/DVL sensor-based navigation filter in the presence of unknown ocean currents. *Automatica, 47*(12), 2604–2614.

Morgado, M., Oliveira, P., & Silvestre, C. (2010, May). Design and experimental evaluation of an integrated USBL/INS system for AUVs. In *Proceedings of the 2010 IEEE International Conference on Robotics and Automation* (pp. 4264–4269). Anchorage, AK.

Morgado, M., Oliveira, P., Silvestre, C., & Vasconcelos, J. (2006, July). USBL/INS tightly-coupled integration technique for underwater vehicles. In *Proceedings of the 9th International Conference on Information Fusion*. Florence.

Rehbinder, H., & Ghosh, B. (2003). Pose estimation using line-based dynamic vision and inertial sensors. *IEEE Transactions on Automatic Control, 48*(2), 186–199.

Ricordel, V., Paris, S., & Opderbecke, J. (2001, March). Trajectory estimation for ultrashort baseline acoustic positioning systems. In *Proceedings of the 2001 Aerospace Conference* (Vol. 4, pp. 1791–1796). Big Sky, MT.

Sabatini, A. (2006). Quaternion-based extended Kalman filter for determining orientation by inertial and magnetic sensing. *IEEE Transactions on Biomedical Engineering, 53*(7), 1346–1356.

Sanyal, A., Lee, T., Leok, M., & McClamroch, N. (2008). Global optimal attitude estimation using uncertainty ellipsoids. *Systems & Control Letters, 57*(3), 236–245.

Sastry, S., & Desoer, C. (1982). The robustness of controllability and observability of linear time-varying systems. *IEEE Transactions on Automatic Control, 27*(4), 933–939.

Tayebi, A., McGilvray, S., Roberts, A., & Moallem, M. (2007, December). Attitude estimation and stabilization of a rigid body using low-cost sensors. In *Proceedings of the 46th IEEE Conference on Decision and Control* (pp. 6424–6429). New Orleans, LA.

Thienel, J., & Sanner, R. (2003). A coupled nonlinear spacecraft attitude controller and observer with an unknown constant Gyro bias and Gyro noise. *IEEE Transactions on Automatic Control, 48*(11), 2011–2015.

Thomas, H. (1998, April). GIB buoys: An interface between space and depths of the oceans. In *Proceedings of the 1998 Workshop on Autonomous Underwater Vehicles* (pp. 181–184). Cambridge, MA.

Vaganay, J., Bellingham, J., & Leonard, J. (1998). Comparison of fix computation and filtering for autonomous acoustic navigation. *International Journal of Systems Science, 29*(10), 1111–1122.

Vasconcelos, J., Cunha, R., Silvestre, C., & Oliveira, P. (2007, December). Landmark based nonlinear observer for rigid body attitude and position estimation. In *Proceedings of the 46th IEEE Conference on Decision and Control* (pp. 1033–1038). New Orleans, LA.

Vik, B., & Fossen, T. (2001, December). A nonlinear observer for GPS and INS integration. In *Proceedings of the 40th IEEE Conference on Decision and Control* (Vol. 3, pp. 2956–2961). Orlando, FL.

Whitcomb, L., Yoerger, D., & Singh, H. (1999, August). Combined doppler/LBL based navigation of underwater vehicles. In *Proceedings of the 11th International Symposium on Unmanned Untethered Submersible Technology*. Durham, NC.